RICE UNIVERSITY

Topological Optimization of Nanofiber Placement in a Continuum
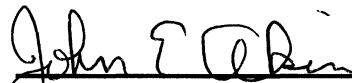
by

Chin-Mow Li

A THESIS SUBMITTED
IN PARTIAL FULFILLMENT OF THE
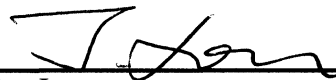REQUIREMENTS FOR THE DEGREE

Master of Science

APPROVED, THESIS COMMITTEE

Dr. John E. Akin, Chair
Professor of Mechanical Engineering

Dr. Andrew J. Meade
Department Chair and Professor

Dr. Jun Lou
Assistant Professor of Mechanical
Engineering and Materials Science

Dr. Andrew J. Dick
Assistant Professor

HOUSTON, TEXAS
December 2011

Abstract

Topological Optimization of Nanofiber Placement in a Continuum

by

Chin-Mow Li

The structural integrity and/or electrical or thermal conductivity of a component can be improved with the optimal topological placement of very high strength or very high conductivity nanofibers. This thesis presents a heuristic procedure for the estimation of the optimal location for the nanofibers based on topological optimization concepts. Previously established topological procedures for continuum-only structures and for truss-only systems are reviewed. Then, this new hybrid approach, which utilizes the continuum model as a retained ground structure, and truss structure for nanofibers, is introduced and evaluated. To initiate this new procedure, a very large number of fiber elements are generated using the material continuum's geometry and then embedded into the component. A finite element method (FEM) program will analyze the structure. Post processing determines which fibers are the least necessary, and deletes them in an iterative process until the desired volume fraction of nanomaterials is reached, leaving only the vital fibers. This procedure is illustrated with several different example geometries and compared to bounding cases from other topological optimization approaches.

Acknowledgments

I would like to thank my graduate adviser Dr. J.E. Akin for providing me with the opportunity to study and research at Rice University, as well as lending me guidance for thesis. This would not have been possible without your patience and support.

I also would like to thank Dr. Andrew Meade, Dr. Jun Lou, and Dr. Andrew Dick for serving on my thesis committee.

Additional thanks go out to Rice University and the University of Texas at Austin for my educational experiences.

And lastly, I want to thank my parents and my sister for their continuous love and encouragement.

Contents

List of Figures

Chapter 1

Introduction

Topology optimization is a concept in engineering design that seeks out the best (or most optimal) solution domain shape, or material placement, for a problem under a set of given circumstances. Evolutionary structural optimization (ESO) is a method in which inefficient material is incrementally removed from a structure in order to improve its efficiency while still retaining optimal functionality. This study will apply the principles of ESO to determine the most ideal placement of nanofibers within a material with the goal of improving its structural integrity, or thermal and electrical conductivity. An algorithm will generate and embed a network of fibers into a geometric solid, which will then be analyzed with the finite element method (FEM). Following the algorithm of ESO (given below), this study will then progressively eliminate those fibers that meet a specific rejection criterion.

1.1. Continuum Components

Evolutionary structural optimization was first conceptualized in 1993 by Xie and Steven [27], who studied instances of shape optimization occurring in nature. More specifically, they noticed that the shapes of structures such as egg shells and animal bones were formed by years of evolution. These structures reached their final state by making incremental adaptations over a large period of time. Xie and Steven applied this concept to engineering: make slight alterations to a solid structure one iteration at a time until an optimal shape has been reached.

The basic ESO algorithm (modified for nanoropes) works as follows:

1. Define domain of ground structure and its boundary conditions.
2. Discretize structure volume into continuum finite elements and insert multiple fiber paths into each continuum element.
3. Perform finite element stress analysis
4. Determine a criteria for deleting fiber elements (continuum elements are unchanged)
5. Post-process all of the continuum and fiber elements to determine their stress or gradients
6. If a fiber element falls below a pre-determined threshold, then delete that element
7. Repeat steps 3-7 until the specified volume fraction of nanomaterials is reached
8. Apply engineering judgment to establish the actual nanorope location.

In 1998, they, along with Li and Querin [19], extended this method to heat conduction problems. Elements that do not contribute to heat transfer (or possess low thermal gradients) within a structure would be deleted. In 2000, Steven, Xie, and Querin [20] published another paper in which they explored ESO's adaptability for different scenarios and developed a number of modifications to improve the procedure. These include:

1. Nibbling ESO - In order to prevent the formation of cavities within the continuum mesh, element deletion is restricted only to those on the boundary of the domain.

2. Bi-Directional ESO - Logic is added to the algorithm such that elements can be added back into the structure if the criterion in an area is above the threshold.

3. Group ESO - Groups of elements are defined prior to finite element analysis. If the group criterion falls below the threshold, then all elements within that group are removed.

4. Stress Minimization - After the initial finite element analysis (FEA) iteration, a virtual load will be applied to the element with the maximum stress. FEA is then performed again, and sensitivity values are calculated. Elements whose sensitivity falls below the threshold are deleted.

5. Multiple Criteria ESO - More than one criterion is defined, and an element will only be deleted if all of its criteria fall below thresholds.

Taskanen [23], in 2002, examined the merits of ESO's theoretical aspects, and concluded that it was a simple yet promising optimization method to be utilized by design engineers.

Hassani and Hinton [14] discuss–various methods of topological optimization in their book. One particular algorithm they detail uses homogenization, a procedure that simulates a composite with many heterogeneities as an equivalent material model, and the optimality criteria method to optimize plane structures via a resizing scheme. These authors also provide a Fortran 77 program named PLATO (PLAne Topology Optimization) that is capable of analyzing plane-stress structures with a host of variables, including material and element types. Figure 1.1 shows a demonstration of PLATO applied to optimize a clamped beam structure with a point load applied to the top right corner. They reduce the effective modulus of elasticity of each element and display that iterative value in a gray scale plot. Thus, all the original elements were retained (which is computationally expensive) and the light gray element are providing some very low level of lateral support for the (black) elements recommended for retention. Such lateral support often leads to hiding kinematic instabilities that would be unacceptable in a real system.

Note here that the two upper left dark regions are in tension, and thus could be enhanced by adding tension fibers. The two lower right regions are mainly compressive and would not benefit from adding tension fibers. Of course, if the design allows for reversals in the load directions, then both regions would benefit from such reinforcements.
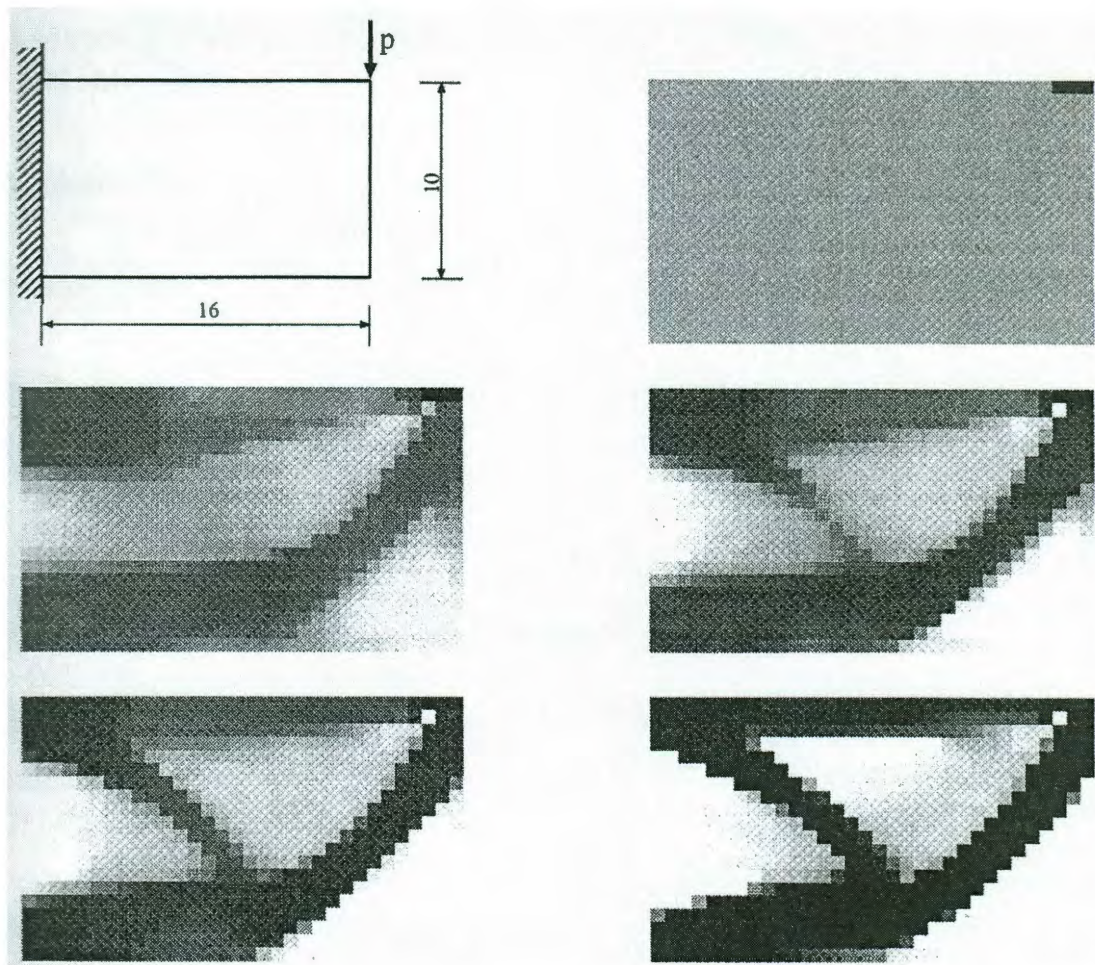
Figure 1.1 - Iteration history of clamped beam example optimized by PLATO

Rozvany [21] delves into the terminology, problem classes, and multiple solution strategies for topology optimization in his essay. He mentions that topological optimization of structures and composite continua consists of two subfields: Layout Optimization (LO), which deals with structures that have low volume fractions, and Generalized Shape Optimization (GSO), which handles higher volume fractions, and

whose solutions may be analytical or based on the finite element method. Within FEM-based GSO, he deems several terms to describe individual elements:

1. Solid (S) - consisting of entirely a single material

2. Empty (E) - void of any material

3. Porous (P) - contains one material and empty space

4. Composite (C) - consisting of multiple materials, but without void

5. Composite-Porous (CP) - consisting of multiple materials and void

He then discusses various problem classes for FEM-based GSO, including Isotropic-Solid-Empty (ISE), Anisotropic-Solid-Empty (ASE), and Isotropic-Solid-Empty-Porous (ISEP) topologies. He also elaborates on three different solution strategies: Solid Isotropic Microstructure with Penalization (SIMP), Optimal Microstructure with Penalization (OMP), and Non-optimal Microstructures (NOM). Between these three solution strategies, Rozvany notes that many researchers consider SIMP to have a number of advantages over other solution strategies, including computational efficiency, versatility, and algorithm simplicity. Meanwhile, OMP and NOM are comparatively disadvantageous due to their more complex natures, their lack of robustness, and requirement for homogenization.

When using traditional continuum elements in topological optimization, problems such as ill-defined boundaries, "checkerboard" patterns, and kinematic instability may arise. Kumar and Parthasarathy [18] investigated the utilization of B-spline approximations in optimization in order to mitigate these irregularities. B-spline elements differ from the usual quadrilateral elements in that they are formed through alternate methods, and are

often of a higher order. After experimentation, they conclude that using B-spline elements in lieu of traditional elements can produce smoother and more well-defined structural shapes. In one example, they apply a topological optimization routine to a cantilever beam with a shear load using various element types. Figure 1.2 displays the domain (a) and compares the optimization results for traditional quadrilateral elements (b and c) to those for B-spline elements (d and e). Note that the latter two results contain fewer isolated elements and have smoother boundary shapes.
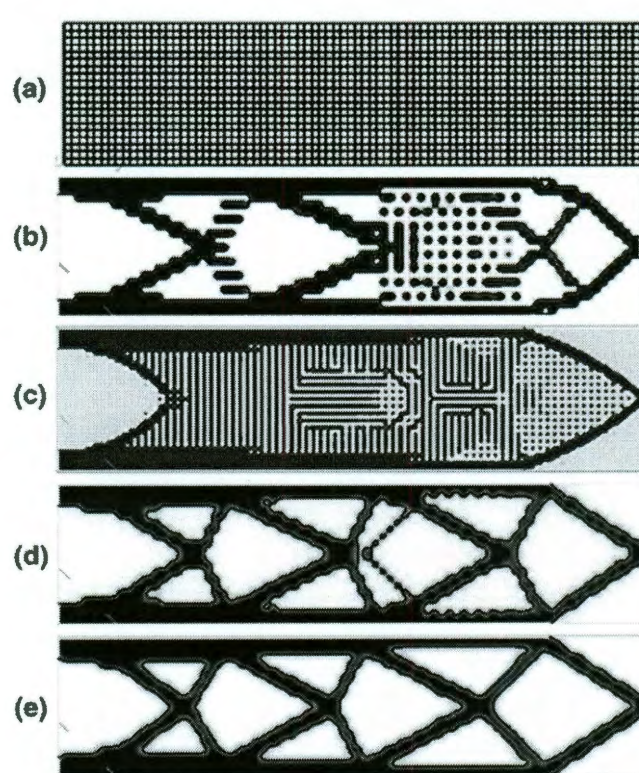
Figure 1.2 - Optimization results for cantilever beam: (a) domain, (b) Quad4N elements, (c) Quad9N elements, (d) B-spline9N elements, (e) B-spline16N elements

1.2. Truss Structures

Hajela and Vittal [13] thoroughly examine the development of stochastic search methods in topological optimization. Their assessment focuses mainly on those methods that employ principles of biological evolution as a foundation. They note that for truss topology, there are a number of methods to utilize genetic algorithms (GA). A genetic algorithm is a search heuristic that mimics natural evolution. A typical GA may proceed as follows:

1. An initial population of randomly generated solutions is defined.

2. Each solution is evaluated and rated for its "fitness", or how close to optimum it is.

3. Through a selection process that favors high fitness, several solutions are chosen to "breed" a new population.

4. Pairs of selected members are "mated" in order to produce a new population generation. Offspring solutions carry traits from their parents, including those that favor optimization.

5. Steps 2-4 are repeated until certain terminating conditions are met.

One evolutionary method for truss topology optimization, explored by Hajela and Lee [12], involves a two-stage optimization procedure:

1. Stage 1 (S1): Through a genetic algorithm, a set of low-weight, kinematically stable truss structures is produced. In this stage, response constraints on stress, displacement, and buckling are not considered.

2. Stage 2 (S2): Using the S1 structures as bases, member resizing is performed, with the goals of minimizing weight and satisfying response constraints. Truss members may be added or subtracted only if the resulting topologies match those identified in S1.

Beckers and Fleury [3] proposed a primal-dual solution scheme for the topological optimization of truss structures. They detail a procedure that first defines an initial "ground structure", and then seeks to select a set of truss members of a certain total volume so that the structure remains kinematically stable. In Figure 1.3, three truss structures undergo this scheme in which each truss has its left corners clamped and a downward point load applied to its bottom right corner. The initial ground structure and final results are displayed for each example.
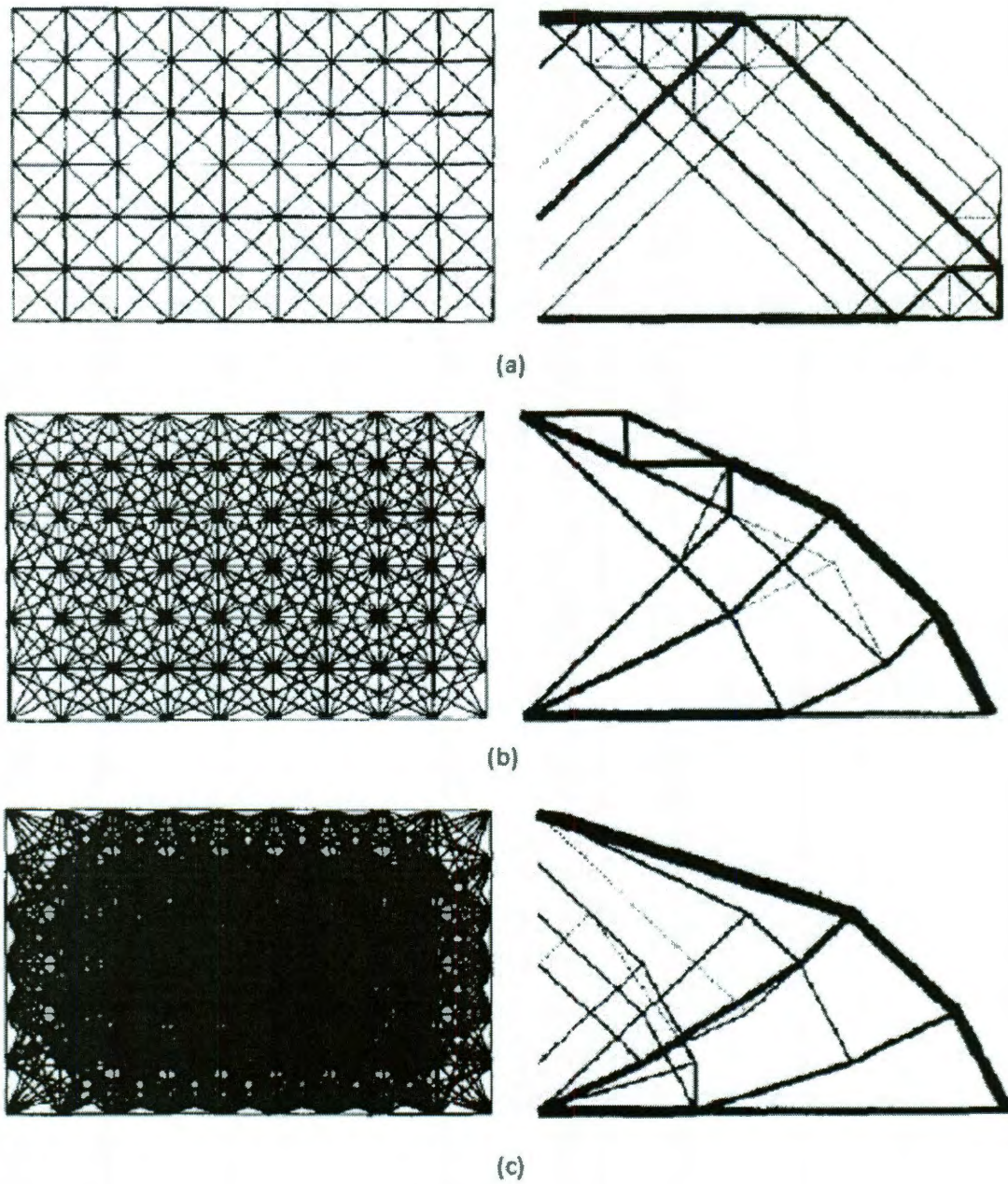
Figure 1.3 - Primal-dual optimization results for truss structures: (a) 225 bars, (b) 411

bars, (c) 701 bars

1.3. Nanomaterials

One key application of nanomaterials is to improve performance and stability of micro- or nano-electro-mechanical systems (MEMS or NEMS). Che, Çağın, and Goddard [5] delved into researching the advantages of using carbon nanotubes for this purpose. They studied how structure, defects, and vacancies can affect the thermal conductivity and found positive results, concluding that the thermal efficiency of carbon nanotubes were comparable to that of diamond crystal and graphite sheet (when a percolation path is formed).

Wu, Natsuki, Kurashiki, Ni, Iwamoto, and Fujii [26] examined the electrical conductivity stability of nano-composite material consisting of carbon nanofiber (CNF) and unsaturated polyester resin (UPR). Their observations and studies concluded that:

1. The CNF/UPR nanocomposites have a low electrical percolation threshold, the critical value where infinite connectivity occurs. This is partly due to the CNF's large aspect ratio.

2. The nanocomposites exhibit the positive temperature coefficient (PTC) effect, where electrical resistance increases with higher temperatures. The influence of temperature is notably more profound near the percolation threshold.

3. The volume resistivity and PTC effect are lower at higher numbers of thermal cycles.

Wichmann [25], in 2011, presented a numerical model to determine and characterize electrical properties of carbon nanotube composites. In this model, a nanotube

microstructure is randomly generated via a Monte Carlo simulation and checked for a percolation path. The generated fibers are converted into a mesh of conducting and contact resistance line elements in order to study its electrical conductivity. A key element of this model is identifying the effective backbone of the conducting network: the percolation path that the current follows from one boundary to the other. This is necessary as the conductivity between the fibers and the material surrounding them differ by a factor in the millions. Figure 1.4 shows a sample resistor network and its effective backbone.
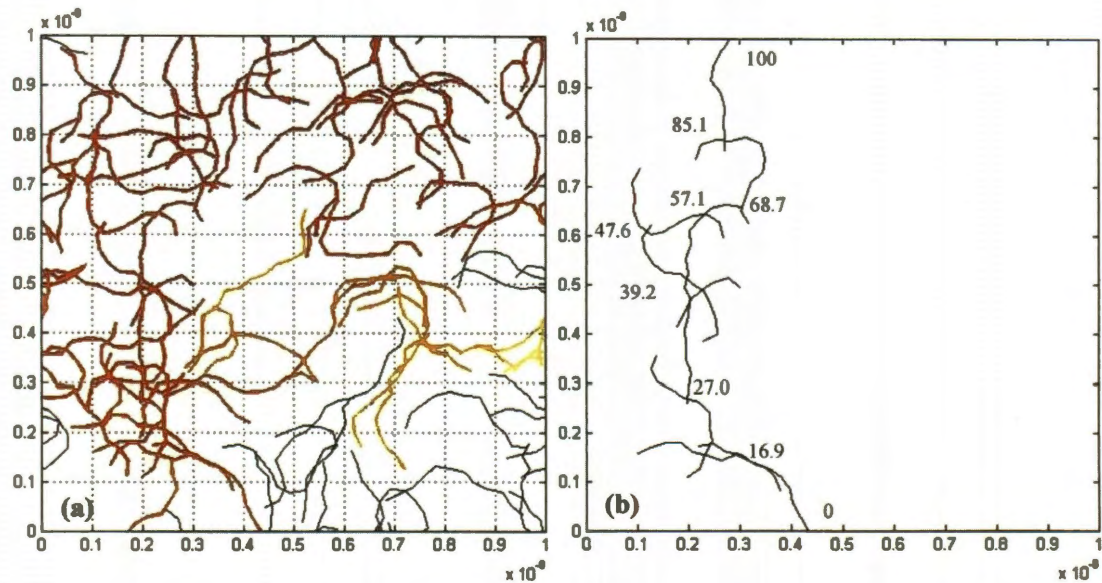

Figure 1.4 - Resistor network (a) and corresponding backbone (b)

In 1998, Islam and Pramila [15] performed a number of finite element analyses of fiber composites with varying temperature and heat flux boundary conditions to estimate their

effective conductivities. They compared the solutions with known experimental and analytical results.

Esteva [10], a graduate student at Rice University, created a model that used the FEM to study the effective elastic and thermal properties of composite material embedded with a specific volume fraction of carbon nanotubes (CNTs). Elsbernd [11] continued that study and extended it to include nonlinear stress analysis.

Zhou and Li [28], in 2006, presented a topological optimization method for fiber-reinforced composite structures under multiple load cases:

1. The fiber-reinforced composite is presented as a material model. The fibers themselves are simulated as members of a truss continuum.

2. The structure undergoes finite element analysis under multiple load cases. The orientation of the fibers are adjusted to match those of the principal stresses, and the fiber densities are altered to be proportional to the strain along those fiber orientations.

3. A group of continuous lines is drawn based on the densities and orientations of fibers at the nodes. A final optimum truss structure can then be formed using the concept as a suggestion.

One of the many examples performed Zhou and Li's study is that of a cantilever beam with two point loads opposite in direction applied at the right end, as seen in Figure 1.5. The beam then undergoes FEA under a specific load case to determine the magnitude and orientation of its principal stresses (as seen in Figure 1.6a), which then serve as a

template for the continuous line mapping (Figure 1.6b), from which the final optimum truss structure (Figure 1.6c) can be determined.
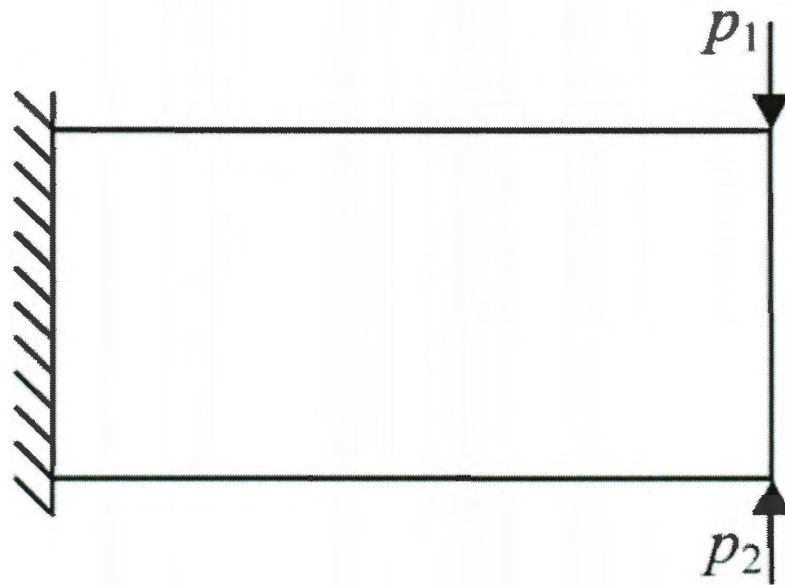
Figure 1.5 - Cantilever beam example for fiber-reinforced composite material model
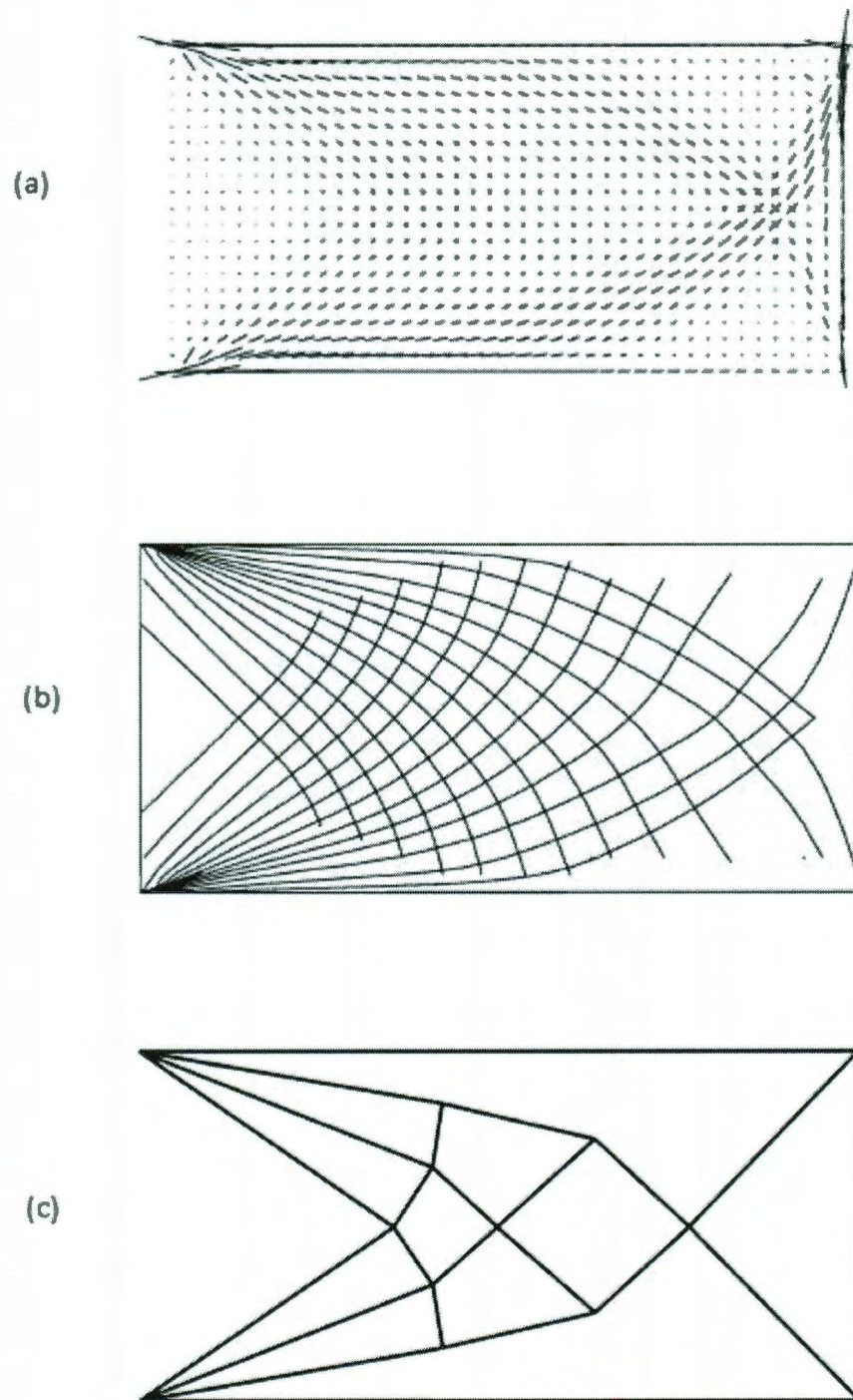
Figure 1.6 - Topological optimization of composite beam: (a) principle stresses, (b) continuous fiber lines, (c) optimal truss

Chapter 2

New Methodology

2.1. Concept

The process developed in this study deals with the placement of nanofibers onto a plane continuum, and the subsequent topological optimization of the fiber network. Unlike Wichmann's model, which produced nano-fibers randomly using Monte Carlo simulations, this methodology employs a procedurally generated nano-fiber network based on the nodal connectivity of the continuum elements.

The interior of an element receives straight fibers that connect between every node on the element. Duplicate fiber elements along the element interface should be avoided. For example, Figure 2.1 shows the effective fibers in 8 node (Serendipity) and 9 node (Lagrangian) quadrilaterals. Elements that contain nodes along their edges are preferable for this type of study not only for improved accuracy, but also to increase the number of fibers initially embedded. For the 8 node element, the four fibers crossing at the center of the element are not connected to each other, and cross over the entire element. For the 9

node element, eight shorter fibers connect to the center node. If the elements are curved the fibers are still straight, but re-aligned to match the node locations on the curve. This process for creating the fiber candidates can be utilized for any two- or three-dimensional continuum element.
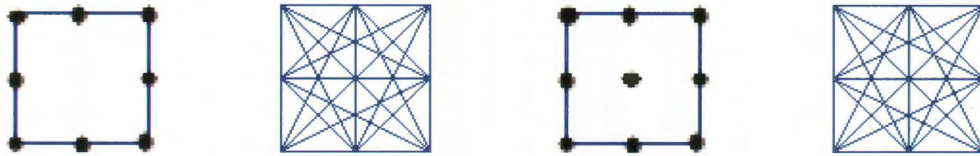
Figure 2.1 – Placement of 24 or 32 fiber elements within each 8 or 9 node quadrilateral

The process of causing the original fiber candidate to connect to the continuum nodes simplifies the linear equations assembly and solution algorithms. It also avoids the use of linear constraint equations to account for the fiber coupling to the continuum material, as was done by Esteva [10] and Elsbernd [9].

The basic algorithm for the topological optimization of the fibers used here goes as follows:

1. The plane structure is defined as a mesh of discrete, two-dimensional continuum elements. In Figure 2.2a, a sample structure is discretized as a continuum of quadrilateral 8-node (Q8) elements.

2. Depending on the node layout, fibers are embedded into each element, as seen in Figure 2.2b (with L2 fiber elements).

3. The structure undergoes the stress or Poisson finite element analysis. For this step, the fiber network is directly coupled to the nodes of the continuum mesh. The fibers act like a constrained truss system.

4. Fiber elements whose strain, or gradient, values fall below a pre-determined threshold are promptly deleted.

5. Steps 3 and 4 are performed iteratively until the specified volume fraction of fibers is reached, leaving only a minimal number of fiber elements remaining.

This methodology can be employed in a number of applications, with various uses including improving the mechanical strength of a structure or the electrical/thermal conductivity of a material.

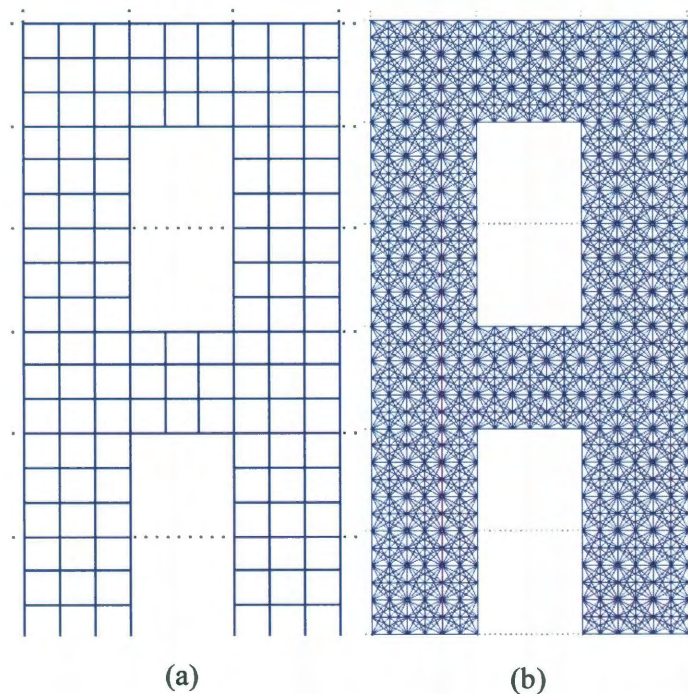(a)   (b)

Figure 2.2 – Structure with (a) Q8 elements, (b) L2 fibers

2.2. Analysis

A brief review of the equations associated with the Finite Element Model for a continuum component imbedded with nanofibers may help understanding the mechanical behaviors and sensitivities of the nanofiber-strengthened structure. For a mechanical component, the stress and thermal analyses use similar equations but with differences: in stress analysis, the displacement response is a vector, while heat transfer produces a scalar temperature response. Furthermore, the ground structure in stress analysis usually experiences external loads as natural boundary conditions (alongside the essential displacement boundary conditions), while in thermal analysis, essential boundary conditions occur in the form of temperatures while the natural boundary conditions involve heat fluxes.

For the quadrilateral element, the element stiffness matrix can be written as an integral over the element area:

$$[S] = \delta \int_{area} [B]^T [E][B] dA \qquad (2.1)$$

Each node has two degrees of freedom in stress problems, and one degree in thermal problems, meaning that the dimensions of the stiffness matrix $[S]$ are $2N \times 2N$ and $N \times N$ respectively, where N is the number of nodes per element. In the preceding equation, δ represents the thickness of the plane element of the ground structure, and $[B]$ contains the derivatives of the shape functions φ_i (x,y) at a location (x,y) inside the element (in which T=1,2,....N). The shape function derivatives are used to convert the nodal response

into response space gradient. The shape function derivative matrix for stress analysis is defined below.

$$[B] = \begin{bmatrix} \frac{\partial \varphi_1}{\partial x} & 0 & \frac{\partial \varphi_2}{\partial x} & 0 & \cdots & \frac{\partial \varphi_N}{\partial x} & 0 \\ 0 & \frac{\partial \varphi_1}{\partial y} & 0 & \frac{\partial \varphi_2}{\partial y} & \cdots & 0 & \frac{\partial \varphi_N}{\partial y} \\ \frac{\partial \varphi_1}{\partial y} & \frac{\partial \varphi_1}{\partial x} & \frac{\partial \varphi_2}{\partial y} & \frac{\partial \varphi_2}{\partial x} & \cdots & \frac{\partial \varphi_N}{\partial y} & \frac{\partial \varphi_N}{\partial x} \end{bmatrix}$$

(2.2)

For thermal or electrical analysis, the shape function is as stated:

$$[E] = \begin{bmatrix} \frac{\partial \varphi_1}{\partial x} & \frac{\partial \varphi_2}{\partial x} & \cdots & \frac{\partial \varphi_N}{\partial x} \\ \frac{\partial \varphi_1}{\partial y} & \frac{\partial \varphi_2}{\partial y} & \cdots & \frac{\partial \varphi_N}{\partial y} \end{bmatrix}$$

(2.3)

In Equation 2.1, $[E]$ is the local stiffness at a given point inside the element. For plain strain, the local matrix relating the stress and strain is a 3x3 matrix given in Equation 2.4, where E_{grd} is the Young's modulus of the ground material, and v is the Poisson ratio of the ground material.

$$[E] = \begin{bmatrix} \frac{E_{grd}}{1-v^2} & \frac{E_{grd}v}{1-v^2} & 0 \\ \frac{E_{grd}v}{1-v^2} & \frac{E_{grd}}{1-v^2} & 0 \\ 0 & 0 & \frac{E_{grd}}{2(1+v)} \end{bmatrix}$$

(2.4)

For heat transfer, the local stiffness matrix relating temperature gradient and heat flux density is described as a 2×2 matrix in Equation 2.5, where k_{grd} is the heat conductivity the ground material.

$$[E] = \begin{bmatrix} k_{grd} & 0 \\ 0 & k_{grd} \end{bmatrix}$$

(2.5)

For a fiber element, the element stiffness is rather straight forward. For stress analysis, it is a 4×4 matrix:

$$[S] = \frac{E_{fib}A_{fib}}{L_{fib}} \begin{bmatrix} \cos^2\alpha & \sin\alpha\cos\alpha & -\cos^2\alpha & -\sin\alpha\cos\alpha \\ \sin\alpha\cos\alpha & \sin^2\alpha & -\sin\alpha\cos\alpha & -\sin^2\alpha \\ -\cos^2\alpha & -\sin\alpha\cos\alpha & \cos^2\alpha & \sin\alpha\cos\alpha \\ -\sin\alpha\cos\alpha & -\sin^2\alpha & \sin\alpha\cos\alpha & \sin^2\alpha \end{bmatrix} \tag{2.6}$$

Meanwhile, the element stiffness for thermal analyses is a 2×2 matrix given as follows:

$$[S] = \begin{bmatrix} \dfrac{k_{fib}A_{fib}}{L_{fib}} & 0 \\ 0 & \dfrac{k_{fib}A_{fib}}{L_{fib}} \end{bmatrix} \tag{2.7}$$

In the proceeding equations, E_{fib}, k_{fib}, A_{fib}, L_{fib} represent the Young's modulus, thermal conductivity, cross-sectional area, and element length of the fiber element, respectively, and α is the orientation of the fiber element with respect to the X-axis.

The $[B]$ matrices for the nanofiber elements are used in post-processing for the transformation from nodal displacement to strain,

$$[B] = [-\cos\alpha \quad -\sin\alpha \quad \cos\alpha \quad \sin\alpha] \tag{2.8}$$

or from nodal temperature to temperature gradient.

$$[B] = [-1 \quad 1] \tag{2.9}$$

An assembly of all of the element stiffness matrices leads to the formation of global element matrix $[K]$. In stress analysis, the nodal responses are the nodal displacements $\{U\}$ under the external nodal loads $\{F\}$ in the ground structure (Equation 2.10), with the

global stiffness $[K]$ assembled from stiffness matrices $[S]$ in Equation 2.1 for ground structural elements and stiffness matrices in Equation 2.6 for fiber elements.

$$\{F\} = [K]\{U\} \tag{2.10}$$

Equation 2.11a then describes the stress vector $\{\sigma(x,y)\}$ in a location in the ground structure as a transformation of the nodal displacement $\{U\}$ through transformation matrices $[B(x,y)]$ and stiffness matrices $[E(x,y)]$, described in Equation 2.2 and 2.4.

$$\{\sigma(x,y)\} = [E][B(x,y)]\{T\} \tag{2.11a}$$

Within the fiber element, the tension T_{en} as a transformation of nodal displacement in a fiber element is provided by

$$T_{en} = E_{fib}\, A_{fib}[B(x,y)]\{U_e\} \tag{2.11b}$$

in which the transformation matrix $[B]$ is given previously by Equation 2.8.

In thermal analysis, the goal is to study the heat conductivity behavior changes caused by the nanofibers. By imposing fixed temperatures to certain nodes as boundary conditions, the temperature distribution at each node can be computed. The result is an essential boundary value problem:

$$\{0\} = [K]\{T\} \tag{2.12}$$

where the global stiffness matrix $[K]$ is an assembly of element matrices $[S]$ taken from Equations 2.1 and 2.7.

The corresponding heat flux density vector $\{h(x,y)\}$ in the ground structure is a transformation of the nodal temperatures $\{T_e\}$ in an element as given by Equation 2.13a,

in which the transformation matrix $[B]$ and element stiffness matrix $[E]$ are derived from Equations 2.3 and 2.5, respectively.

$$[b(x,y)] = [E][B(x,y)]\{T\} \tag{2.13a}$$

The total thermal flux H along the fiber line is given by

$$H = k_{fib}\, A_{fib}[B]\{T_e\} \tag{2.13b}$$

While electrical components may physically differ from mechanical ones, the mathematical model for electrical computation bares many similarities to that of thermal computation. The basic differential equations for heat flux field (heat flux density distribution, denoted by $\vec{h}$) and electrical current field (current density distribution, denoted by $\vec{\imath}$) are the gradient of temperature ($\vec{\nabla}T$ in Equation 2.14) and voltage ($\vec{\nabla}V$ in Equation 2.15) respectively.

$$\vec{h} = k\vec{\nabla}T \tag{2.14}$$

$$\vec{\imath} = \kappa\vec{\nabla}V \tag{2.15}$$

Let the electrical conductivity be denoted by κ. Electrical conductivity is the inverse reciprocal of the electrical resistivity. The electrical resistance is related to the electrical conductivity, as seen in the following equation:

$$R = \frac{L}{\kappa A} \tag{2.16}$$

The finite element formulation for electrical analysis of a quadrilateral element is then provided by Equation 2.17, where $[B]$ is calculated from Equation 2.8, and κ_{grd} is the electrical conductivity of the ground material.

$$[E] = \begin{bmatrix} \kappa_{grd} & 0 \\ 0 & \kappa_{grd} \end{bmatrix} \tag{2.17}$$

The formulation of element stiffness of a nanofiber element is then represented by Equation 2.18.

$$[S] = \begin{bmatrix} \dfrac{\kappa_{fib}A_{fib}}{L_{fib}} & 0 \\ 0 & -\dfrac{\kappa_{fib}A_{fib}}{L_{fib}} \end{bmatrix} \tag{2.18}$$

The other equations are similar to their thermal counterparts. The global equation is

$$\{0\} = [K]\{V\} \tag{2.19}$$

Where the global stiffness $[K]$ is the assembly of element stiffness matrices $[S]$ form Equations 2.1, 2.8, 2.17, and 2.18, and $[V]$ is the global vector for nodal voltages.

The electrical current per unit area $i(x,y)$ in the ground structure is given from the nodal voltages within an element:

$$\{i(x,y)\} = [E][B(x,y)]\{V\} \tag{2.20a}$$

with $[E]$ and $[B]$ coming from Equations 2.17 and 2.3, respectively.

For the fibers, the electric current along the fiber line (denoted by I) is given by

$$I = \kappa_{fib}\, A_{fib}[B]\{V_e\} \tag{2.20b}$$

Chapter 3

Structural Applications

3.1. Shear Wall Structure

The text by Hassani and Hinton gives several structural examples. In one particular problem, the shear-wall structure in Figure 3.1 has its bottom edges clamped, and is given two horizontal point forces: the first one is at the top-left corner, and second is at the left-side midpoint.

First principle stress contours for this example (before fibers are introduced) are given in Figure 3.2 in which red marks regions of the highest tension and blue denotes areas that lack tension or experience compression. Note that it is assumed that the ground material can resist high compressions, but limited tension stresses. The compression force distribution is not of interest in this study.
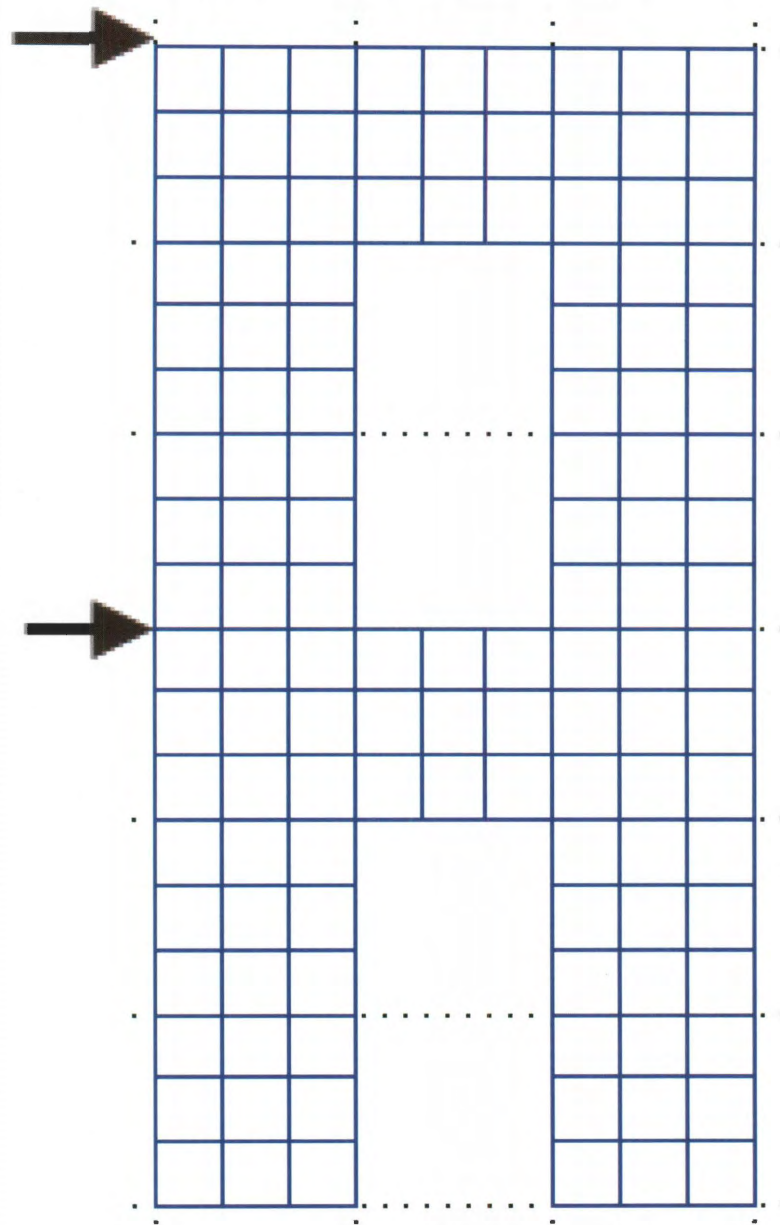
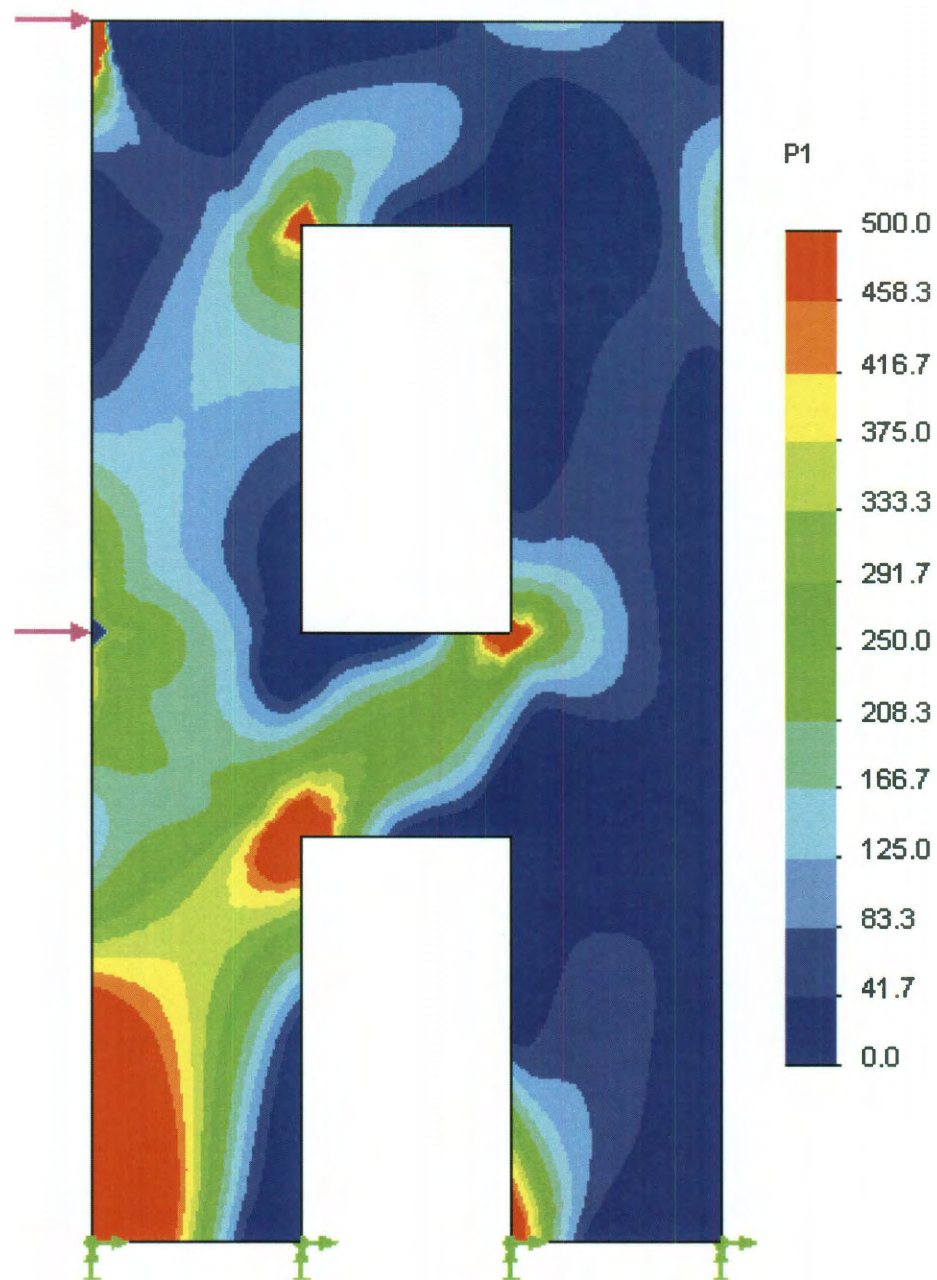Figure 3.1 - Shear Wall Structure

Figure 3.2 - Stress Contour of Shear Wall Structure without Fibers

Once the nano-fibers have been implanted, the optimization method will delete low-tension fibers and fibers in compression until a threshold is reached. The deletion process was, in this case, carried out over a series of eight iterations, and is terminated when the specified volume fraction is reached. This process is shown in Figures 3.3 and 3.4, where red indicates fibers that have yet to be eliminated. Blue lines are fibers that have been deleted. Figure 3.5 provides an enlarged view of the final retained fibers in comparison to the final stress contour mapping. Note that when compared to original fiber-free mapping (Figure 3.2), the final solution with the embedded fibers experiences considerably lower levels of stress.

That figure shows a coupled continuum-fiber system with two basic fiber group paths. The lower (diagonal) group tends to follow the highest region of tension found in the continuum only model. The second group of fibers lie along the left structure edge. Being similar to a cantilever beam, experience shows that the original structure would have flexural tension stresses on the left and compression on the right side. Thus, the selected path would seem to be an improvement over the continuum material alone.
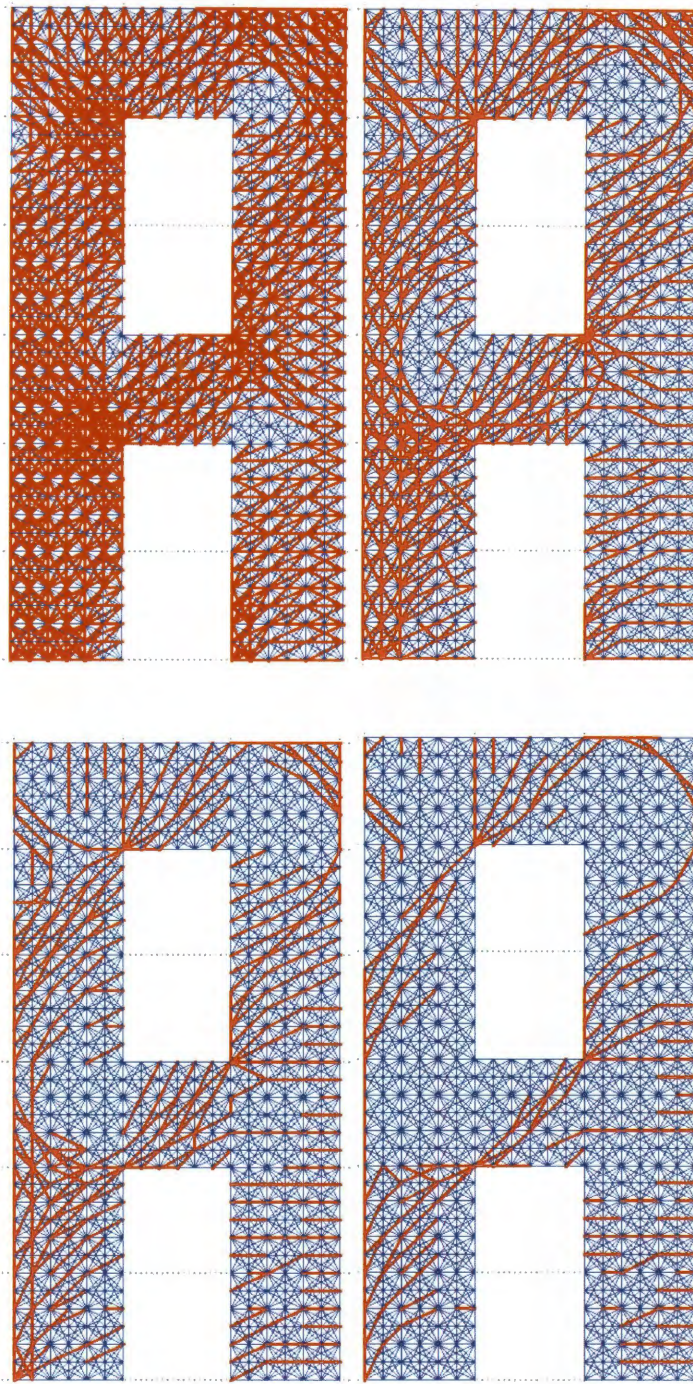
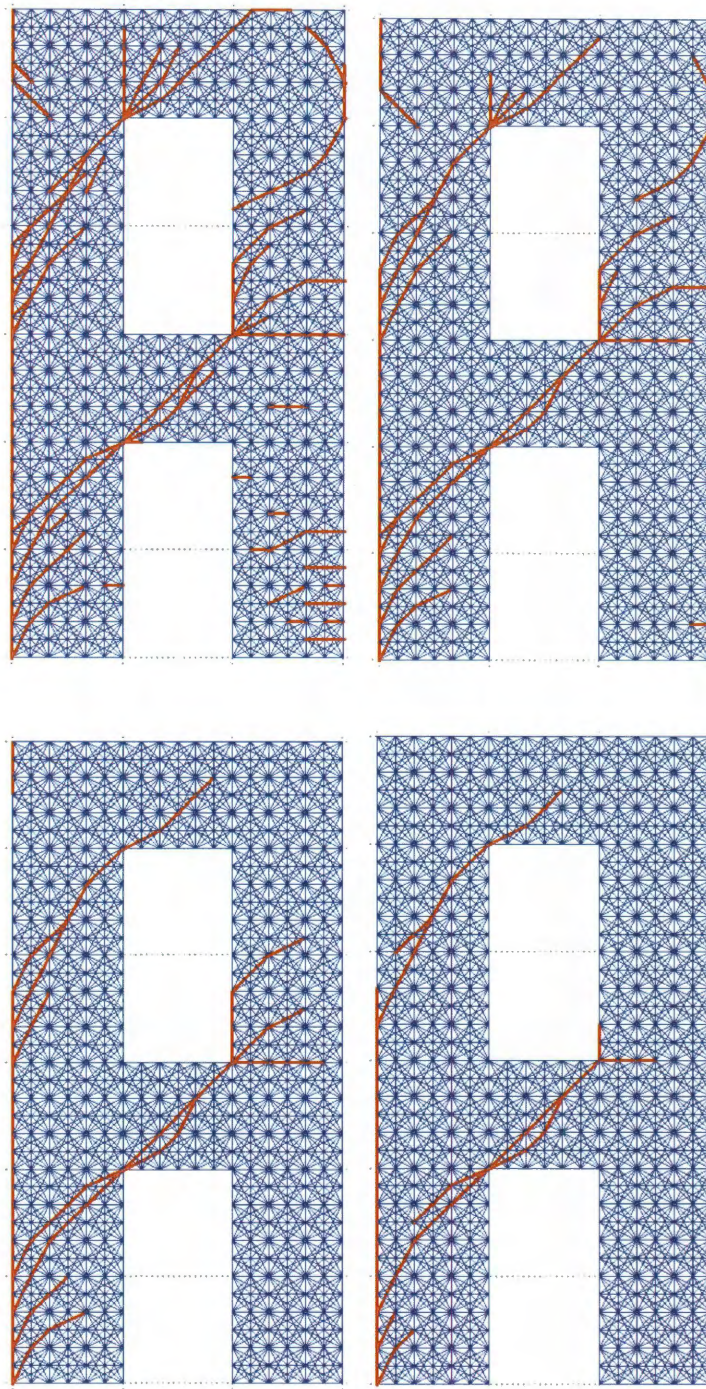Figure 3.3 - Blue deleted and red retained fibers of first four (of eight) stages

Figure 3.4 - Blue deleted and red retained fibers of last four (of eight) stages

Figure 3.5 - Final Retained Fiber Groups

The stage 3 and 4 plots of Figure 3.3 illustrate a potential disadvantage of the current fiber deletion logic. There it is apparent that in some positions a single fiber has been retained, even though it was not connected to any other retained fiber. If the part were produced by rapid prototype printing that could be done. However, if an actual series of continuous fibers are to added to the continuum, then retaining such fibers is undesirable. Retained single fibers are still counted in the volume fraction of reinforcing or conducting materials. For electrical applications with extremely high conductivity fibers

it is important to retain a percolating path. That importance on a continuous path of connected fibers renders lone fibers nearly useless.

The mesh database contains information on all elements connected to each element. Thus, it would be practical to add another loop to the deletion process that would determine if a retained fiber is surrounded by deleted fibers. If so, that single fiber would be deleted. Since the quantity of fibers is quite large, such an additional search should be delayed until the first few iterations have deleted a large percentage of the fibers.

As mentioned earlier, this problem was solved with the PLATO system in an effort to define a truss system that could carry the imposed loads while satisfying the geometric restraints for avoiding the hole regions. The resulting optimal system is seen in Figure 3.6. The black elements (on the right) are the retained continuum elements from the original continuum design region. Those elements are supported by hidden continuum elements whose elastic modulus has been reduced by about a factor of a million. The string of continuum elements would be replaced by a single truss (line) element. The final set of continuum elements is kinematically unstable since some are connected only at their opposite corners. If the hidden elements were not retained, then the continuum model would have been singular and no stress results could have been retained.

Similar to how final continuum meshes are converted to trusses, the retained coupled fibers of the current approach would probably be further revised by fitting a continuous fiber (spline) through all of the retained fibers. That calculation has not been done for the examples being presented here, but it would be easy to "eyeball" such a path and then do a final analysis using a continuum with such a fiber path(s).
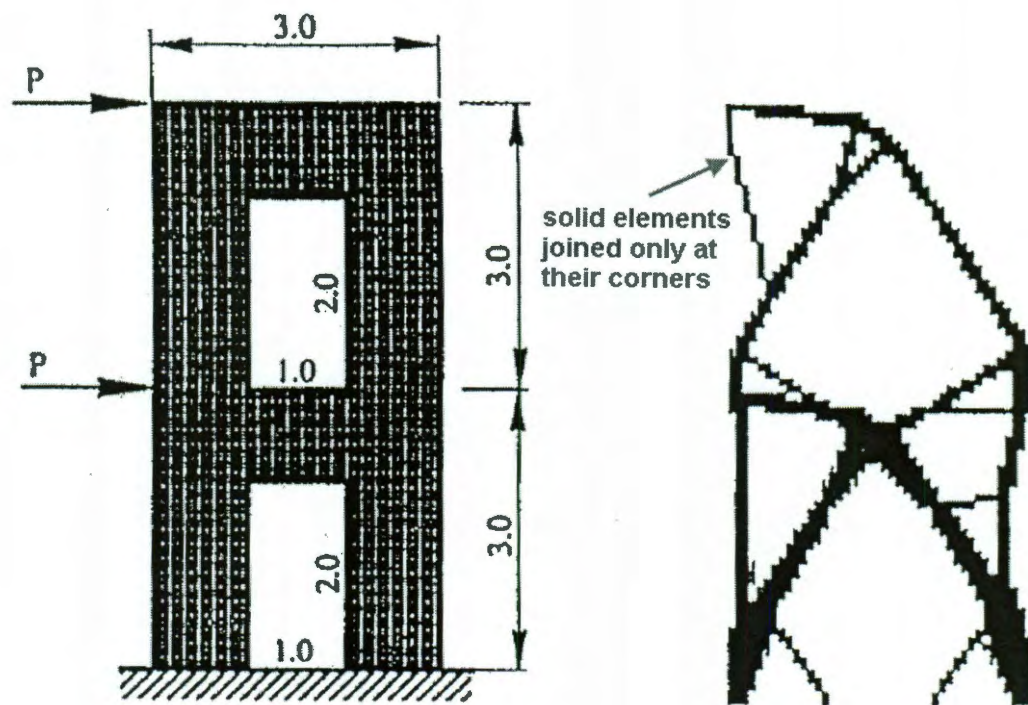
Figure 3.6 - PLATO Approximate Equivalent Truss System

3.2. Beckers and Fleury Cantilever

In another example, the truss that Beckers and Fleury used to demonstrate their primal-dual scheme (from Figure 1.3) is modeled as a continuum plate. For this problem, the continuum is discretized into 60 Q8 elements initially embedded with 1,232 L2 fiber elements (Figure 3.7).
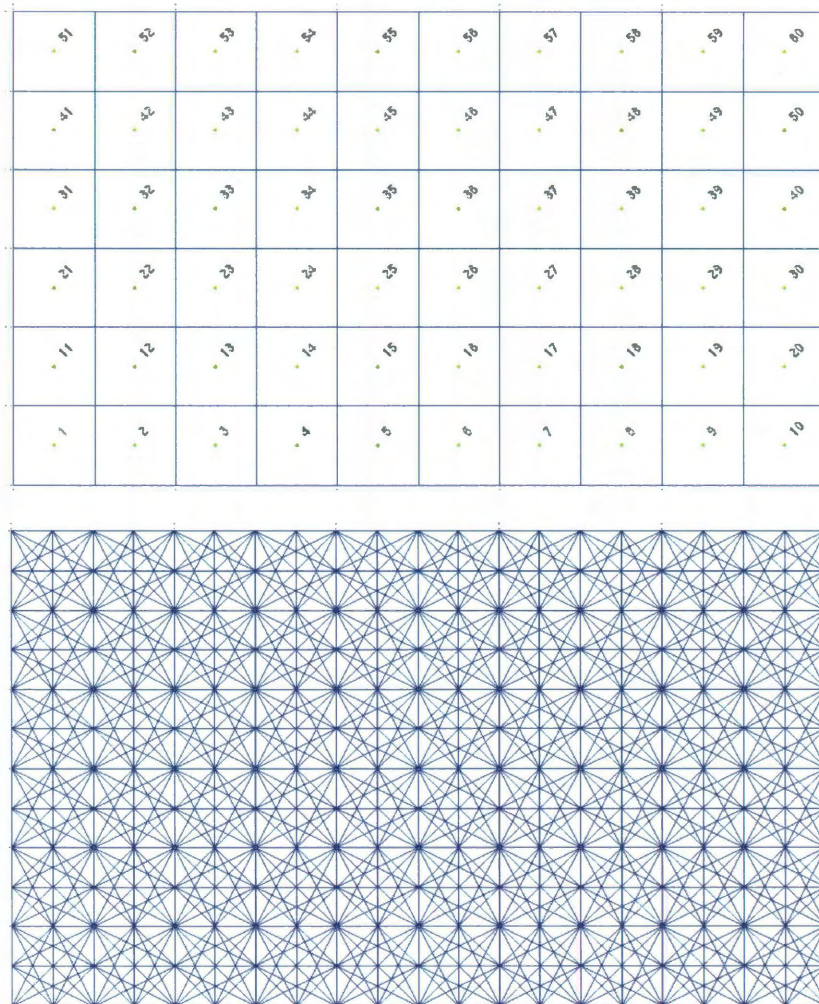

Figure 3.7 - Continuum and initial fiber elements for a cantilever supported on the left

For finite element analyses, two different cases are examined. In case (1), the entire left edge of the structure is clamped, and a point load is applied to its bottom right corner. The iterative history leading to its final result is displayed in Figure 3.8.
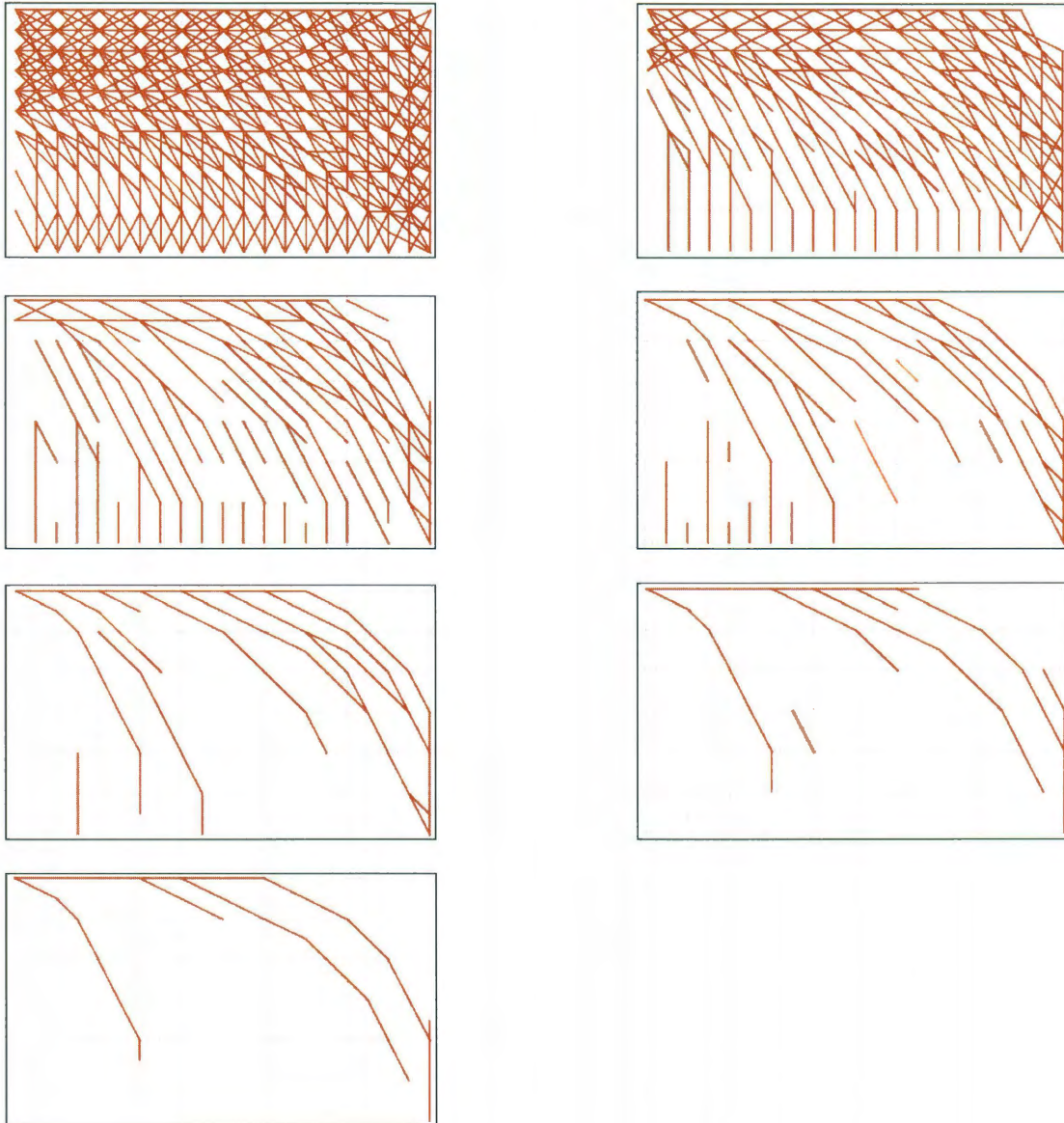

Figure 3.8 – Seven stages of retained ribers for corner point load case

For case (2), the force is represented differently. Rather than as a single point load, the applied force is modeled as three forces distributed equally among the lower edge of the bottom right quadrilateral, see Figure 3.9. As can be seen in Figure 3.10, this alteration will result in a slightly different solution. In both cases the desirable fiber path appears to run along the top edge for about half the length, and then arcs downward to the centroid of the load region.
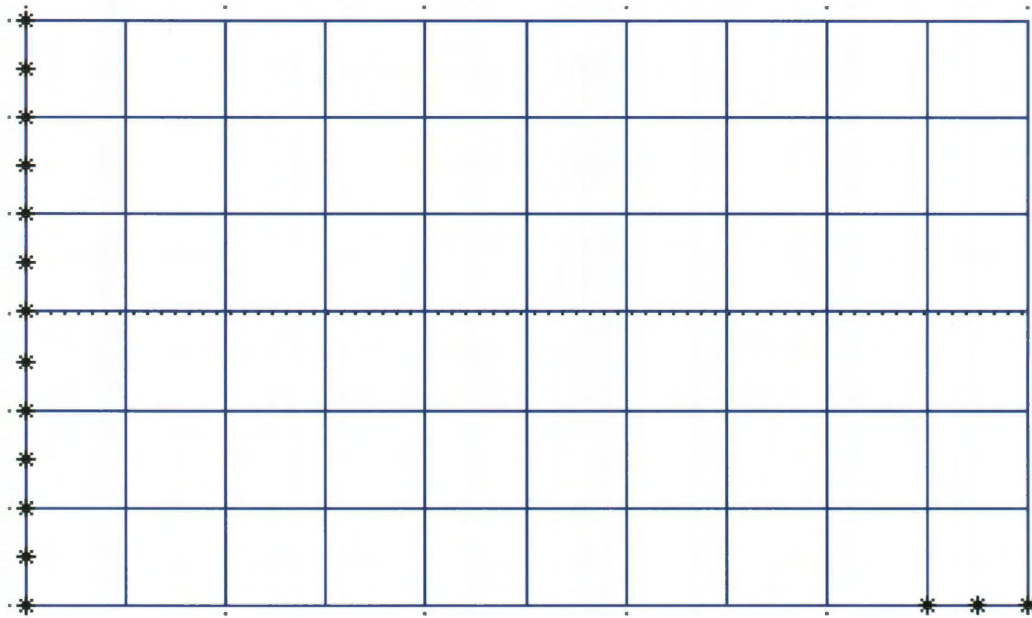
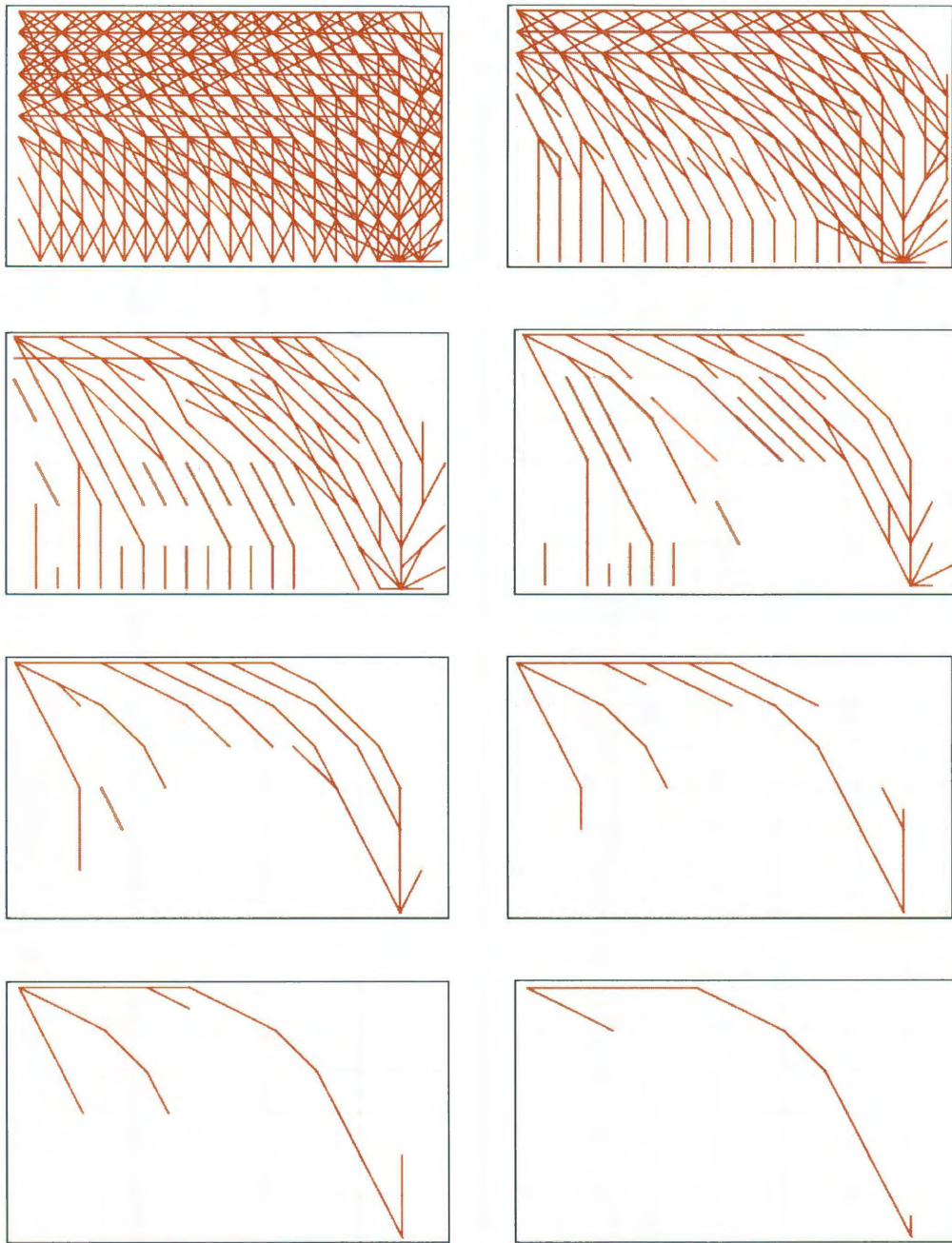Figure 3.9 - Supported (left) and loaded (right) nodes

Figure 3.10 – Eight stages of retained fibers for edge load case

The equivalent truss developed by Beckers and Fleury had both tension and compression members (and none of the original continuum elements). Thus, their result, in Figure 3.11, shows a completely different optimal structure. Since the current process retains all of the original solids in a part or solid design it is different from the other approaches considered in the literature.
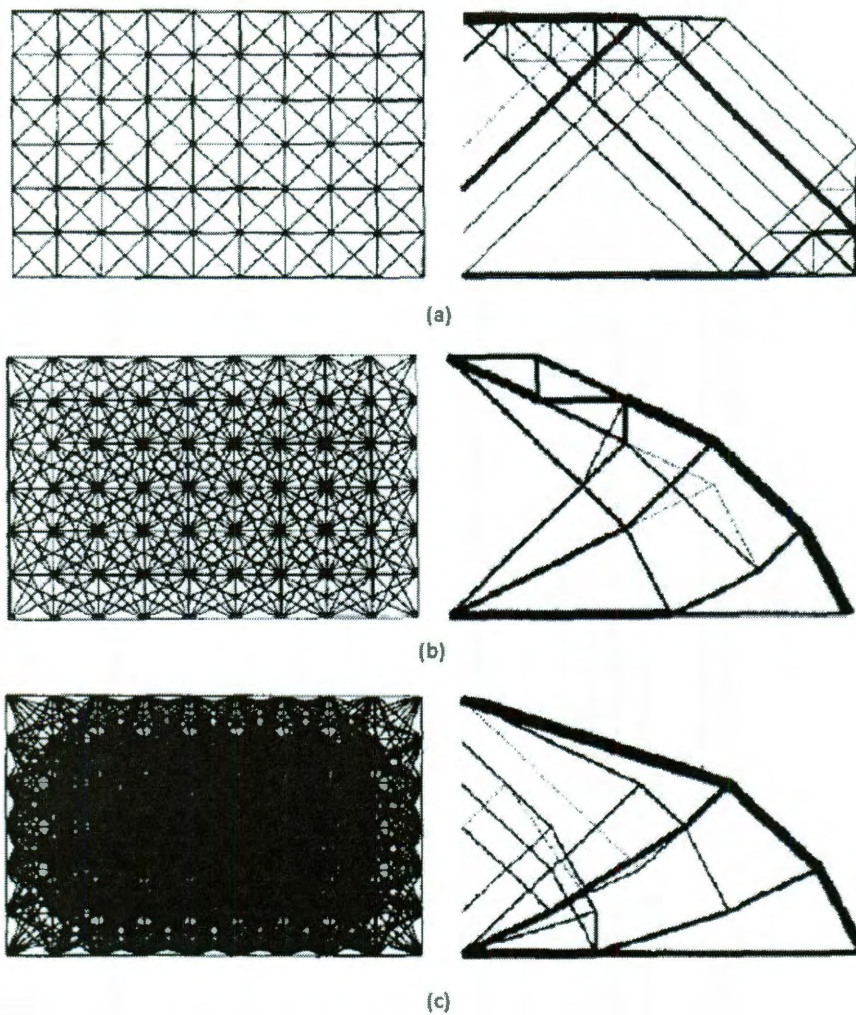
(a)

(b)

(c)

Figure 3.11 - Beckers and Fleury optimal trusses for case 1

3.3. Rectangular Plate with Hole

Here is a more irregular structural example, involving a rectangular design place with a circular hole at its center, where no material exists. The plate is supported at its left boundary, and is given an upward vertical load at its top-right corner. This example was originally used as a demonstration of PLATO in Hinton and Hassani's work. The problem design, along with two optimal solutions (obtained using different criteria), is illustrated in Figure 3.12 below.

For this study, the design region serves the geometry for the continuum element mesh in which fibers are imbedded to as reinforcement. Figure 3.13 shows the original mesh, as well as the contours for first principle (P1) stress and Von Mises stress for the solution without fibers. The iteration history for the retained fibers is given in Figures 3.14 and 3.15. Note that the arrangement of the retained fibers does seem to follow the original PLATO solutions, as well as the P1 stress contours.

In Figure 3.16, a zoomed in scan shows that the solution does not manage to retain a perfect percolation path, as there is an undesired gap. Were this an electrical problem, it would be critical to rectify this (possibly by fitting a single continuous fiber through the retained elements), as the entire solution would fail. This figure also shows a free-standing fiber as well as two connected fibers isolated from the main path.
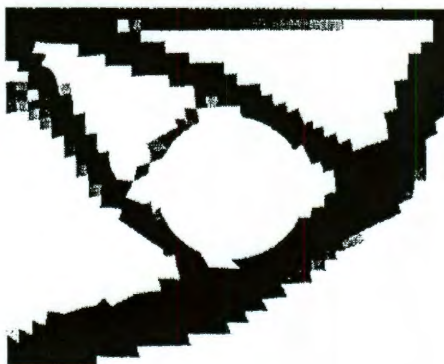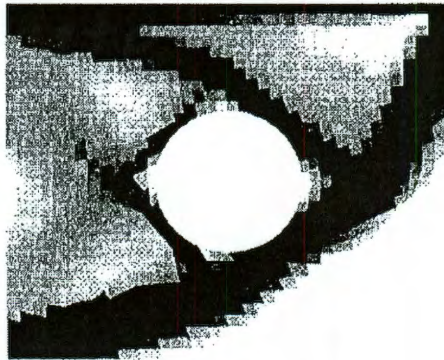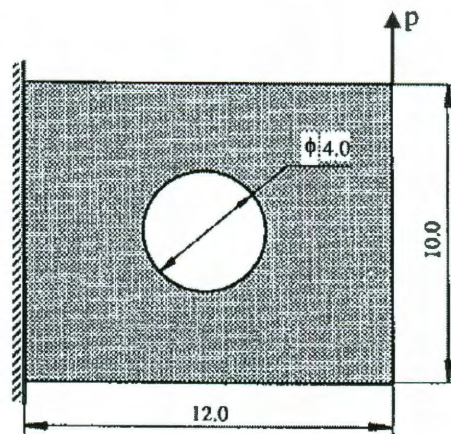
Figure 3.12 - Rectangle with hole design, and two optimal solutions
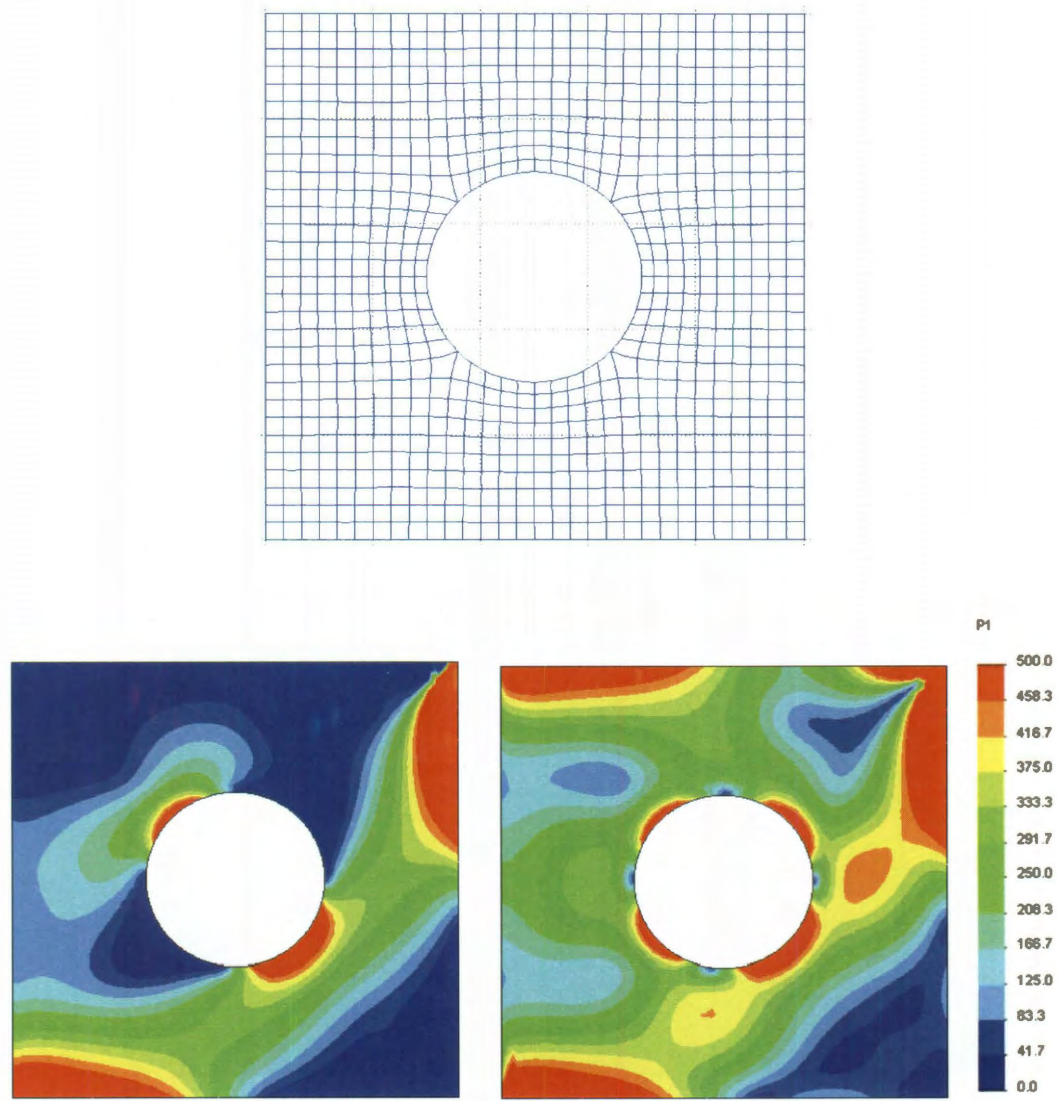
Figure 3.13 - Continuum mesh (without fibers), with P1 and Von Mises stress contours
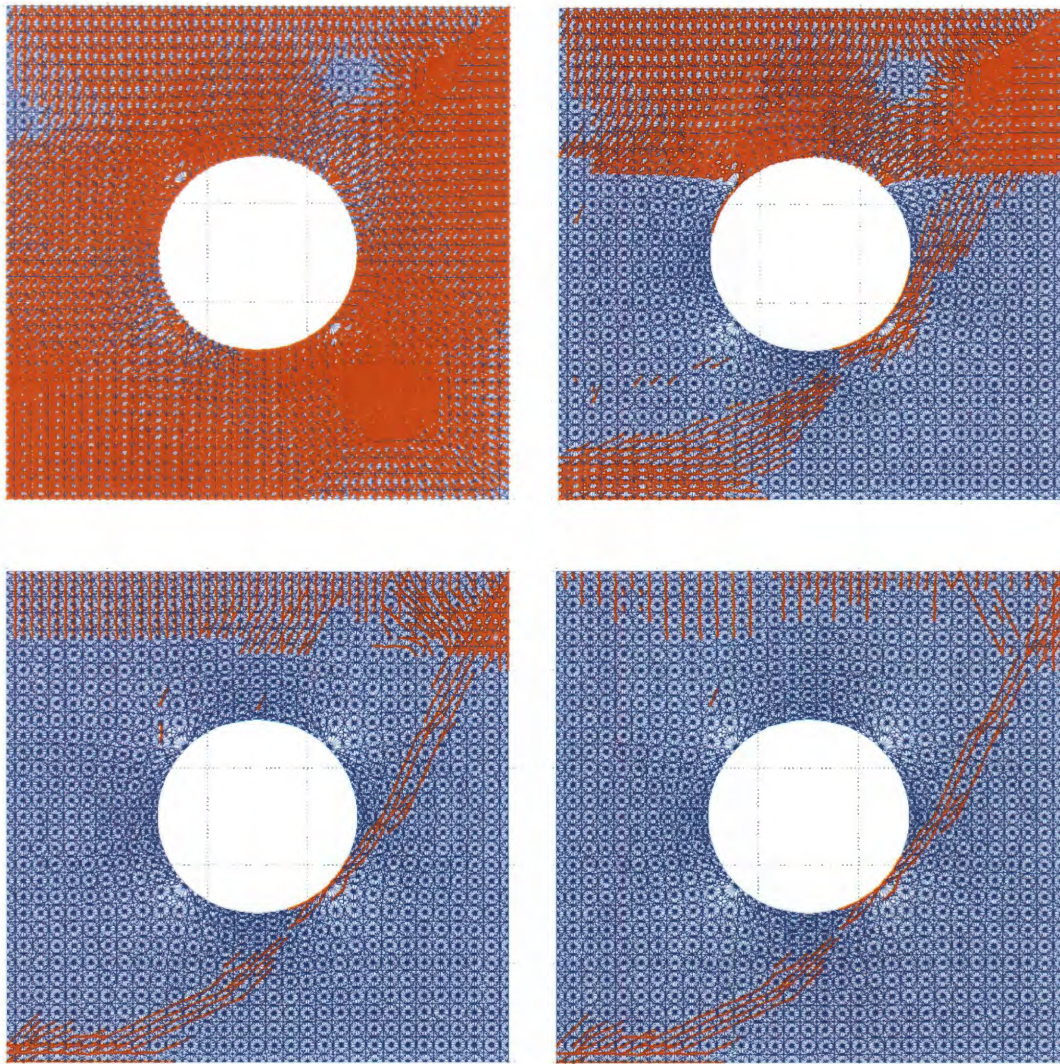
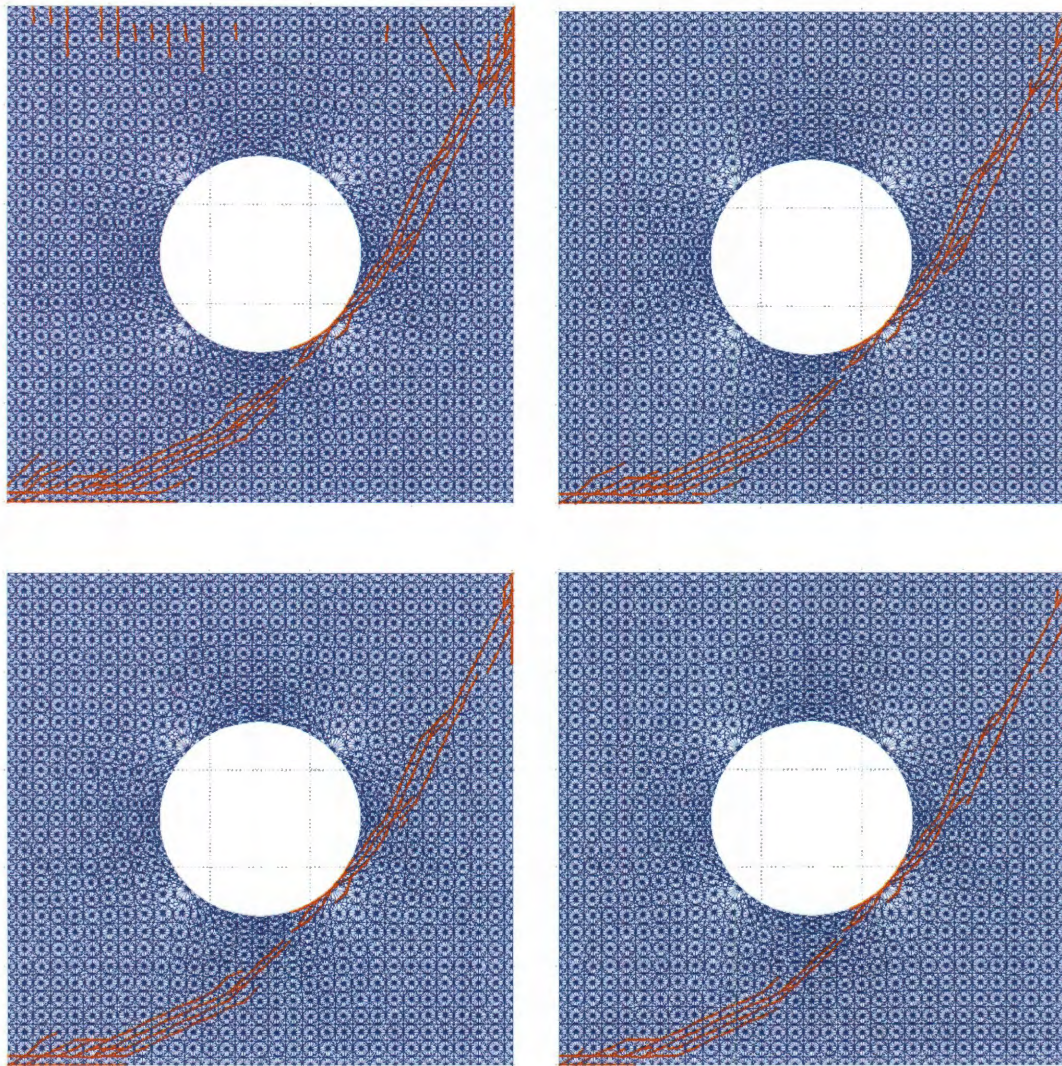Figure 3.14 - First four (of eight) iterations of retained (red) fibers

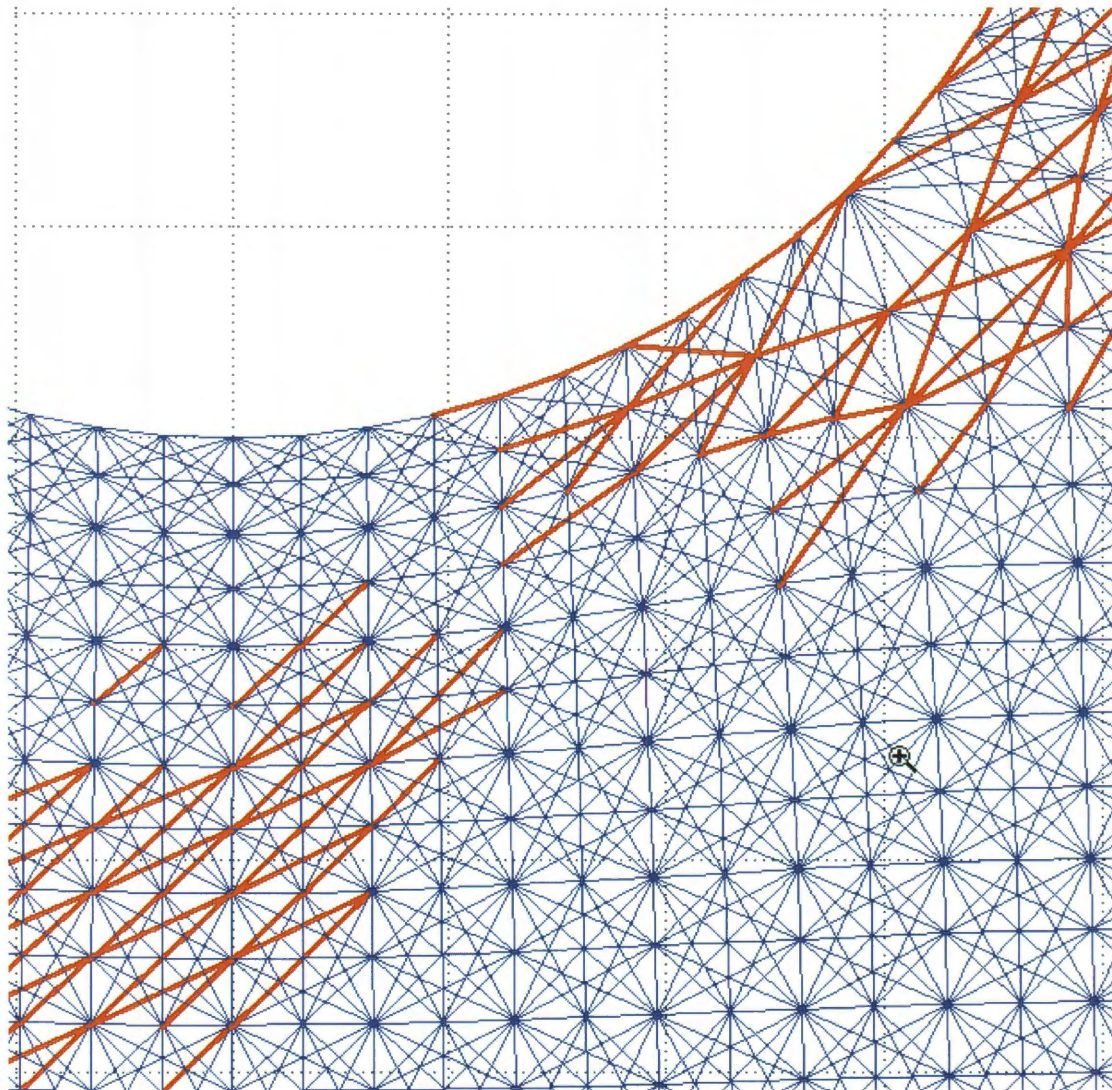Figure 3.15 - Final four (of eight) iterations of retained (red) fibers

Figure 3.16 - Loss of percolation path due to gap between retained fibers

3.4. Isolated Fiber Elements

As seen in Figure 3.16, and in the thermal applications that follow, the final solution of an optimization problem solved under the initial deletion logic method may leave single or double fibers floating in an otherwise empty region of the continuum, separated from the main fiber path. Such elements provide very little to no functionality in stress relief or thermal/electrical transfer. One suggested improvement would then be to implement a routine that would identify and eliminate isolated fiber elements. One way to accomplish this is to store a database that lists each fiber's neighboring elements, and delete those that have zero or only one neighbor. That is a relatively fast search process. Extending such a "clean up" process in each iteration becomes prohibitively expensive when applied to paths with only three of four fiber members.

At the end of this research the "clean up" algorithm was implemented and it successfully eliminated paths with only one or two fibers. Thus, it did give a better distribution of the final volume fraction. However, having a more concentrated group of fibers in the final state still did not prevent gaps from developing in the final fiber paths. An example of this is given in Figure 3.17. That figure shows the re-run of the previous example with the "clean up" algorithm turned on. In the zoomed region near the bottom of the circular hole the bold black lines show where free standing fibers had appeared in Figure 3.16. While the single and two fiber paths were eliminated, a gap in the total fiber space still developed.
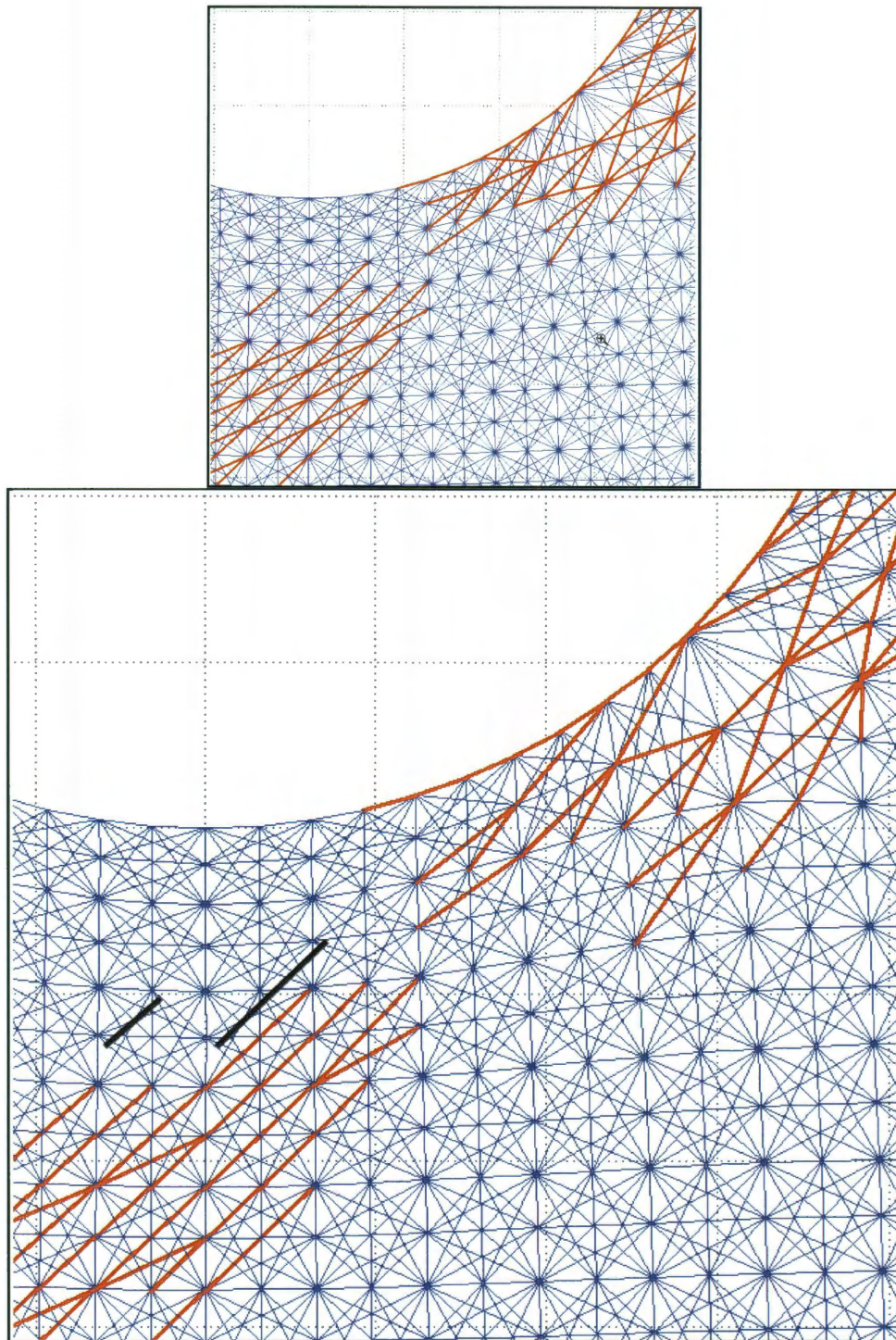
Figure 3.17 - Loss of percolation path due to gap with "clean up" turned on

Chapter 4

Thermal Applications

4.1. Heat Transfer Example Case 1 - Fibers Initially Omitted

Once again using the geometry and mesh in Figure 2.2a, a structure comprised of 8-node quadrilateral elements is given a specified temperature (essential boundary condition) along its bottom left edge, and a heat flux applied to its upper right corner. The linear two noded (L2) thermally conducting fibers are embedded into the continuum, as seen in Figure 2.2b.

There are multiple approaches used for this particular example. In Case 1, the fibers are not present initially. Only after the first finite element analysis iteration are the fibers inserted into the structure. The primary thermal contour for this case is given in Figure 4.1, and the iterative optimization history is recorded in the following Figures 4.2 and 4.3.
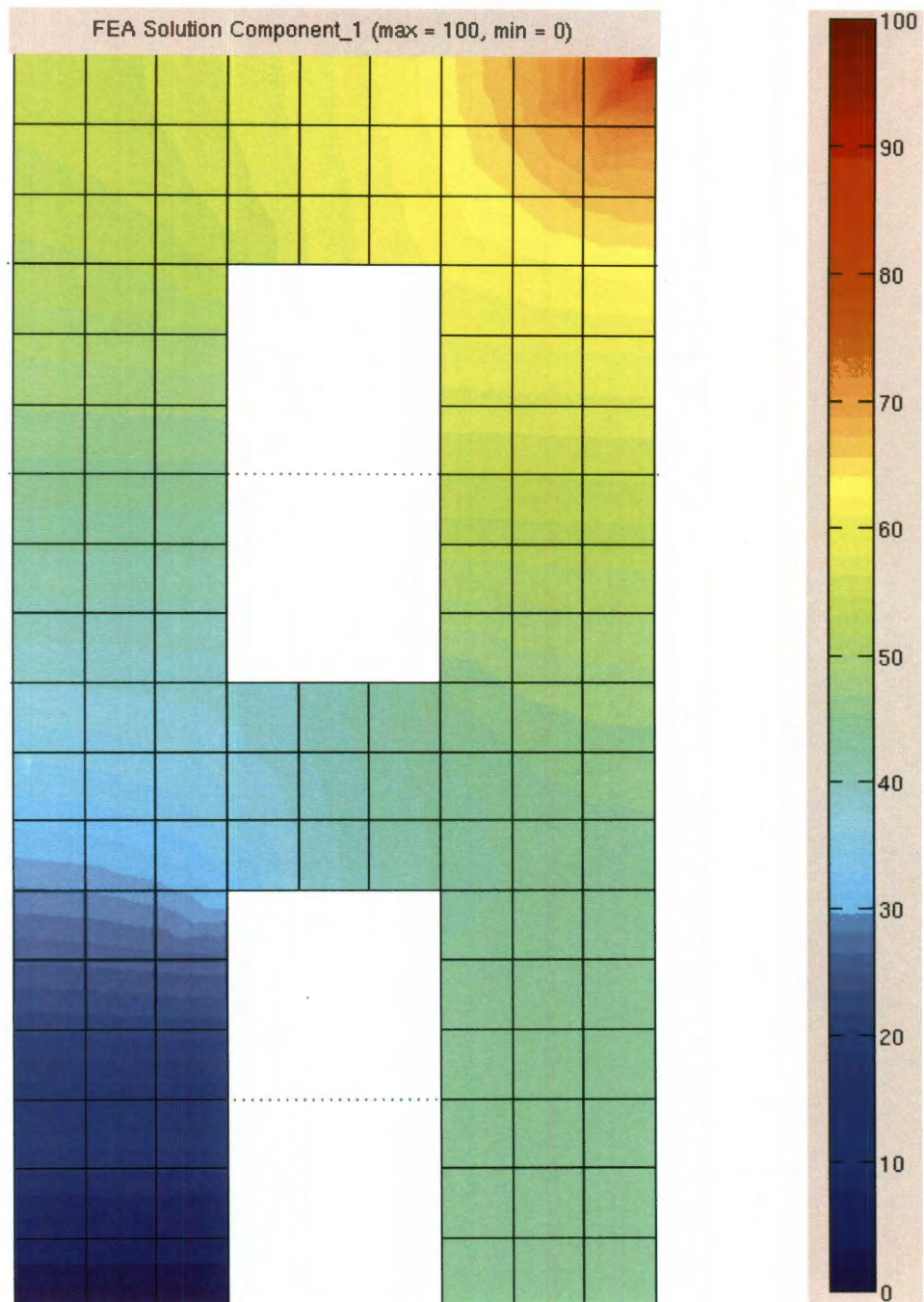
Figure 4.1 - Continuum temperature contour for Case 1 (no high conductivity fibers added)

Figure 4.2 - First three (of six) iterations of retained fibers for thermal example Case 1

Figure 4.3 - Final three (of six) iterations of retained fibers for thermal example Case 1

4.2. Heat Transfer Example Case 2 - Fibers Initially Present

In Case 2 of this example, the nanofibers are applied during the first iteration of FEA, and remain throughout the whole procedure. Figure 4.4 compares this case's thermal contour to that of the previous one, while Figures 4.5 and 4.6 illustrate the iteration history. Note that for both cases, the final results for both schemes are similar, and each is able to effectively produce a percolation path from the flux point at the top right to the bounding on the bottom left edge.
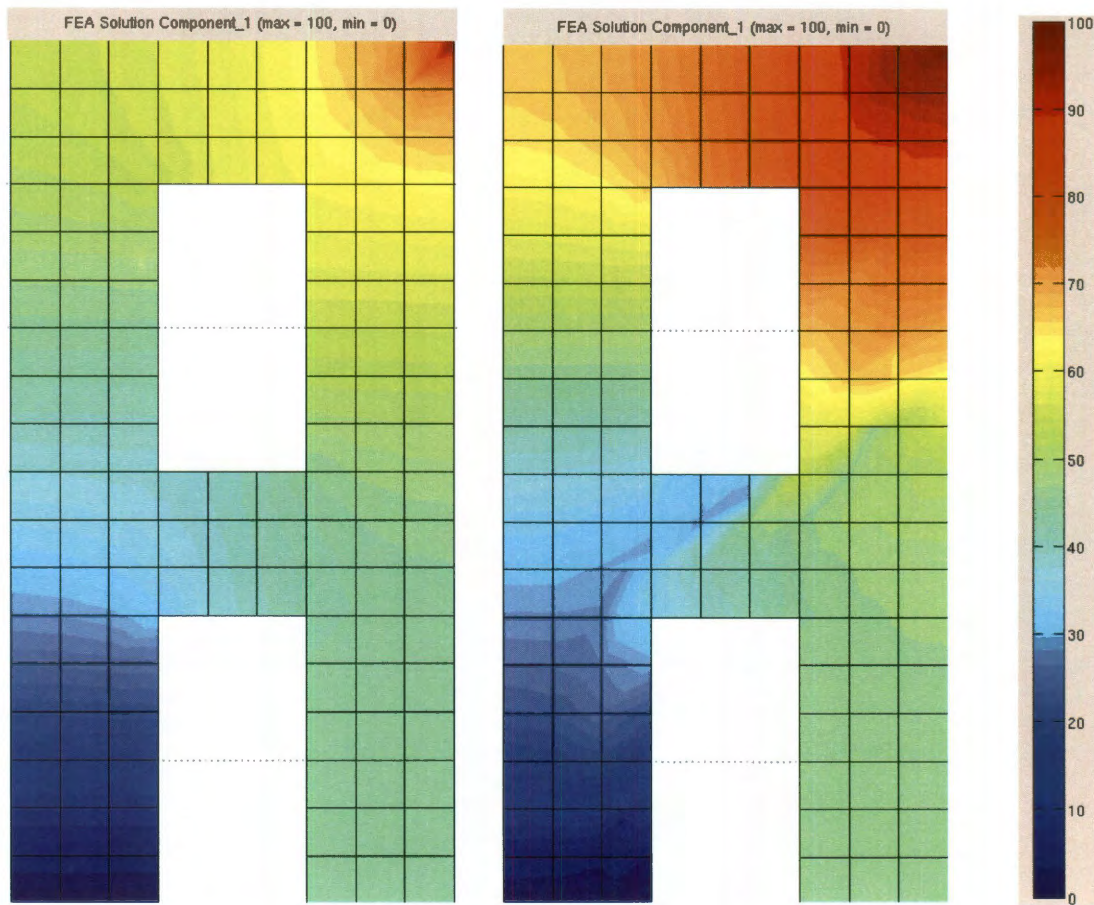
Figure 4.4 - Continuum temperature contours for Case 1 (left) and Case 2 (right)
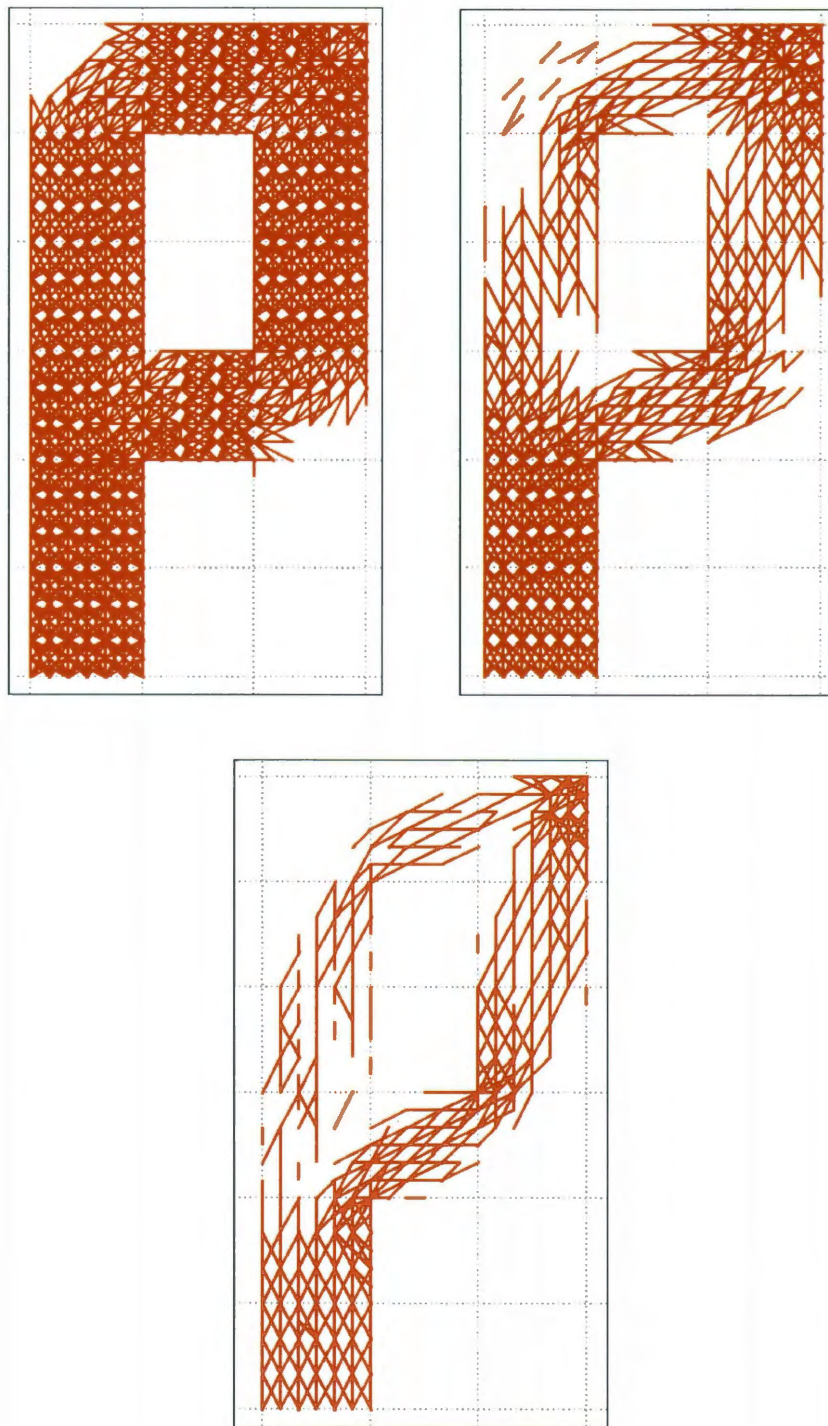
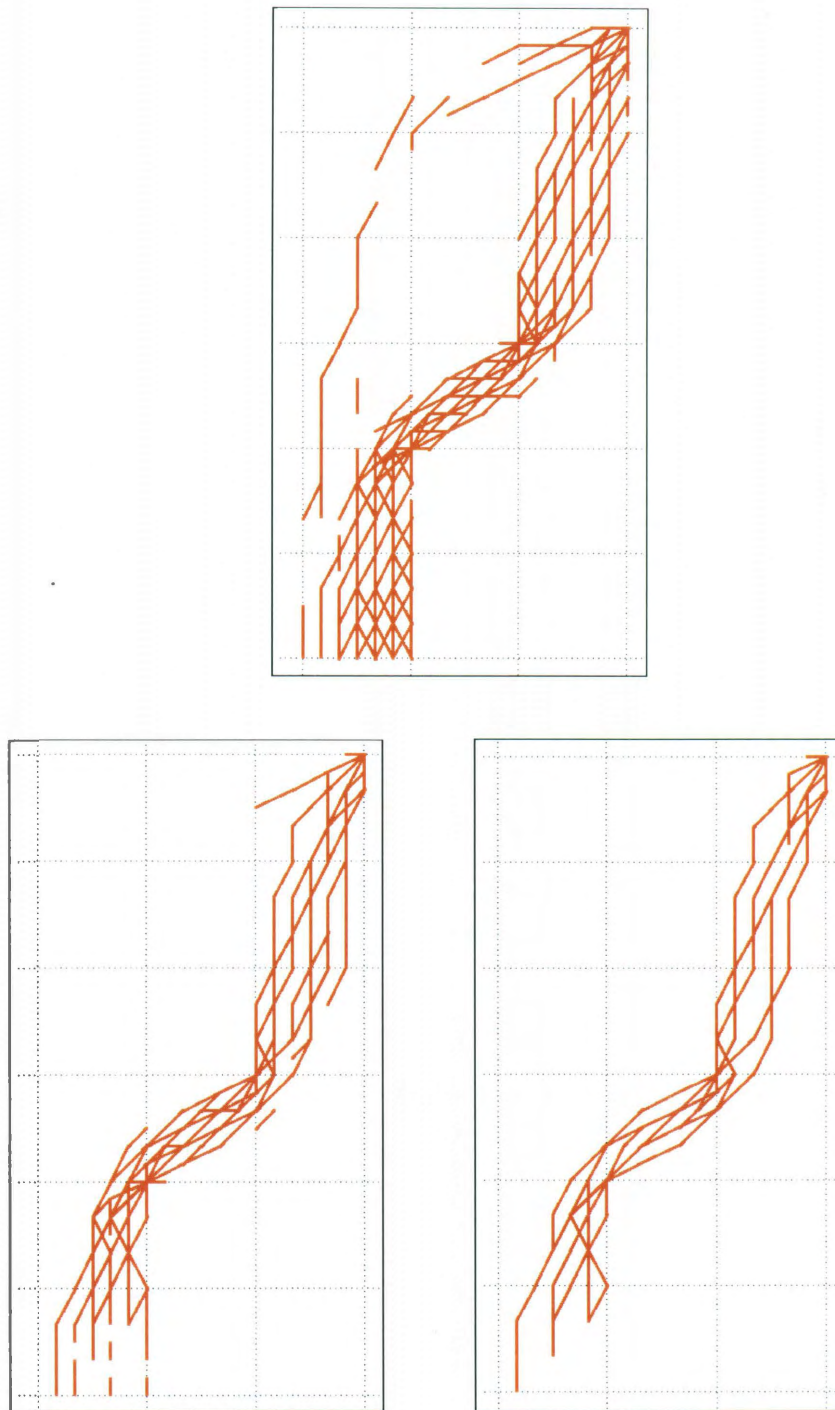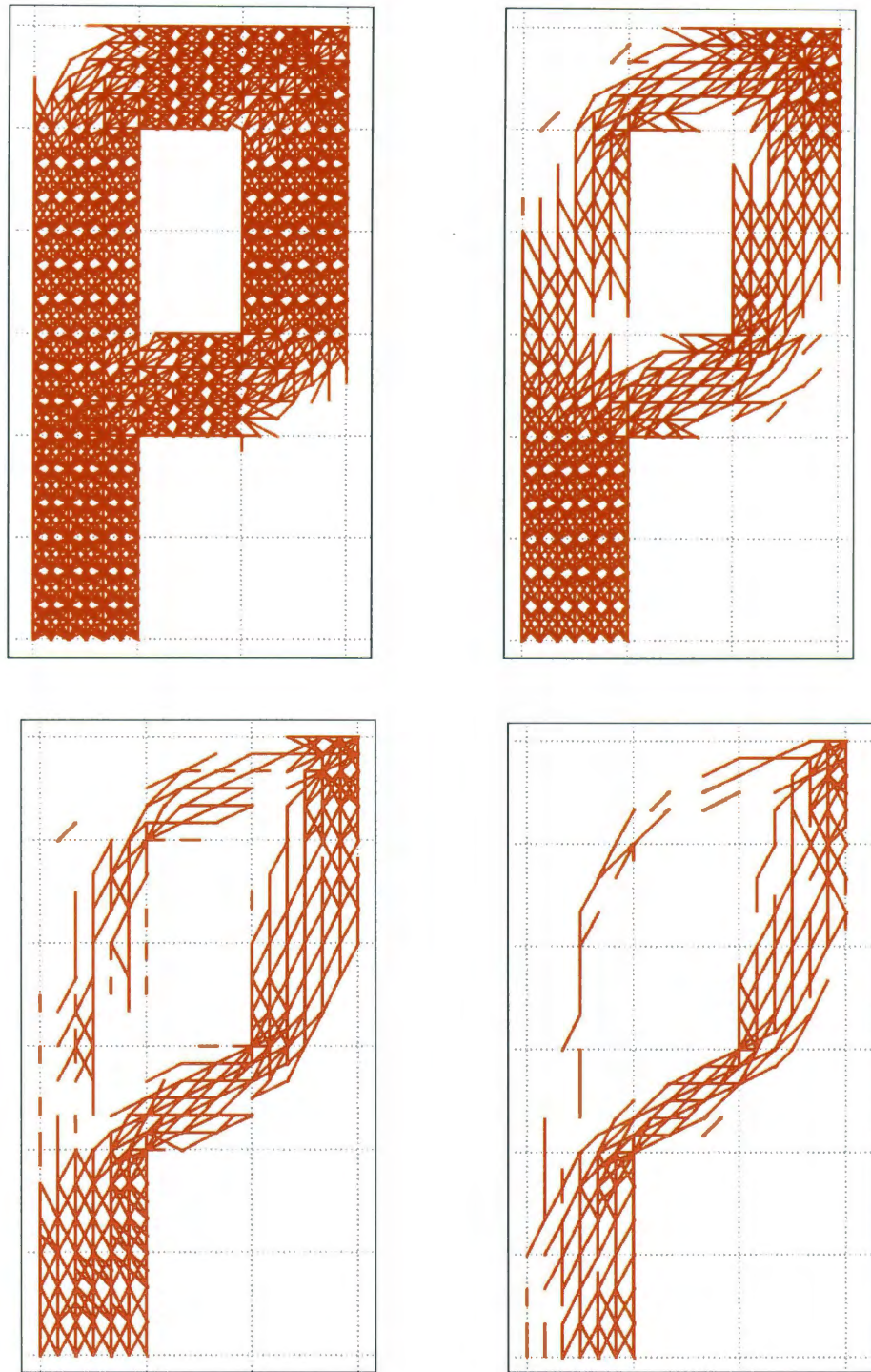Figure 4.5 - First four (of seven) iterations of retained fibers for thermal example Case 2
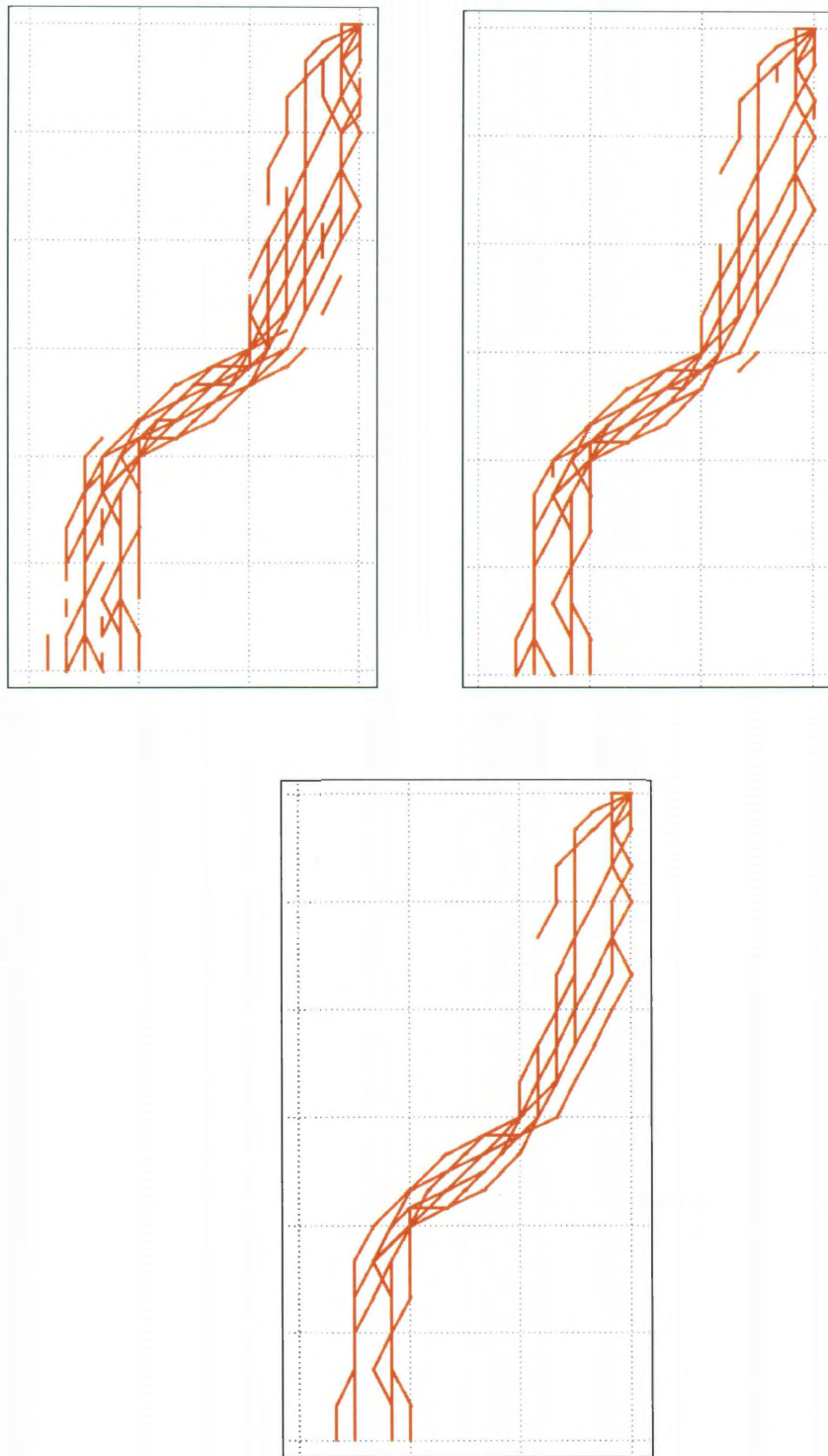
Figure 4.6 - Final three (of seven) iterations of retained fibers for thermal example Case 2

4.3. Heat Transfer Example Case 3 - Heuristic Approach

Upon completion of the initial study using the crude mesh, it is possible to use heuristic evaluation to refine the continuum mesh and/or limit the region where fibers are applied. In case (3) of the same previous example, the fibers are embedded only in the space where the percolative path (judging from previous results) is expected. The refined mesh and selected fiber network are shown in Figure 4.7. The temperature distribution is nearly identical to that of Case 2 (in Figure 4.4).
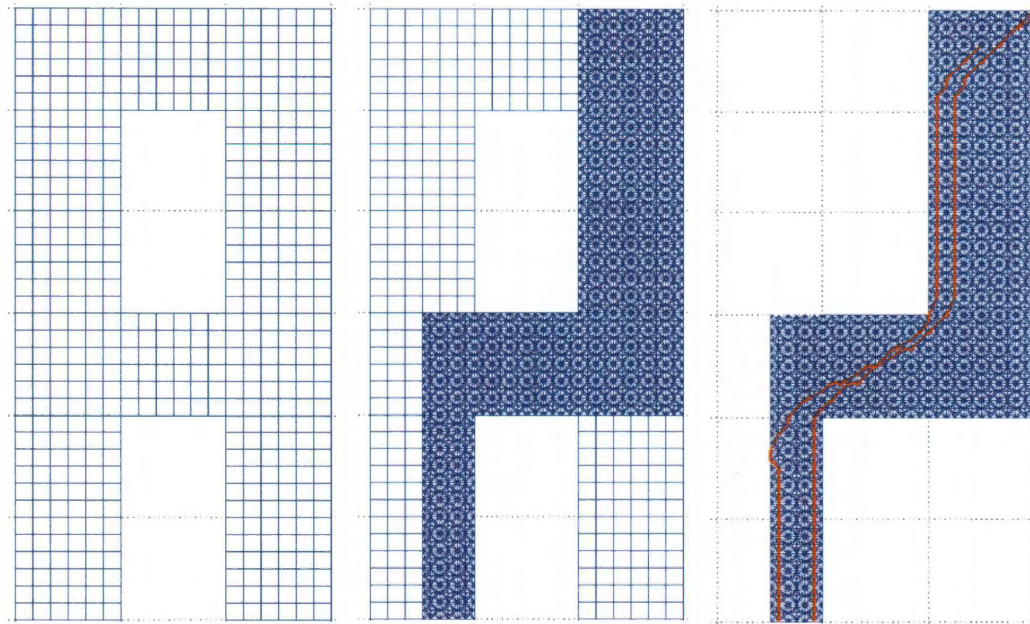
Figure 4.7 - Continuum mesh, fiber network, and optimal results for thermal example

Case 3

Chapter 5

Electrical Applications

5.1. Introduction

For electrical applications one has the same governing equations as for the thermal applications presented previously. The critical difference is that the electrical conductivity of the fiber can be thousands or millions of times larger than the thermal conductivity value. The huge electrical conductivity of the fibers causes numerical ill-conditioning in the electrical application that was not present in thermal and structural applications. That is because round off error makes the polymer material essentially vanish and the electrical fibers function as if suspended in a vacuum. That is, unless some of the fibers form percolation paths between locations of essential boundary conditions, or from an input source to a location of an essential boundary condition, the equations become singular and no solution is obtained. In the electrical application percolation paths can also be formed by electron tunneling, as discussed by Wichmann [24]. When fibers get within a specific distance of each other a tunneling resistance is overcome and electrons can flow between them. That is, the conducting fibers do not

always have to be physically connected to form percolation paths. However, a set of one-dimensional "tunneling elements" would have to be inserted into the original mesh so that some of their nodal connectivity's close the gap(s) in a percolation path.

5.2. Maintaining an Unbroken Percolation Path

In the present implementation, it is important for the final solution to keep a continuous nanofiber path connecting one boundary of the structure to another, especially in electrical engineering cases, where the high conductivity of the fiber elements relative to the continuum would cause the system to become singular. Wichmann's work on numerical modeling of nanocomposite electrical properties discusses this in detail. Normally, the initial fiber mesh by default includes a huge number of potential percolation paths. Logic could be implemented to check that the no gaps will be formed in the path before each respective fiber is killed.

In some cases, gaps can form as the result of the fiber path branching out in two or more different directions, only to rejoin at a different location. This can result in the algorithm severing the path by deleting both branches. To prevent this occurrence, the methodology must be altered so that it can recognize these situations, and ensure that one of the branches is spared so that the percolation path is not broken.

When all else fails, and gaps in the percolation path still exist despite the system checks proposed above, there is always the contingency of simply "fixing" said gaps by adopting the bi-directional evolutionary structural optimization discussed by Steven, Xie, and Querin previously. If the algorithm is able to identify what would otherwise be a perfect

path save for a few missing links, then it could simply add the fibers back in. However, this solution should be a last resort only, and needs to be heavily refined so that it doesn't recreate extraneous fiber elements.

The current approach initially creates a very large number of conducting fibers on top of the continuum mesh. It would be too expensive to search all of the distances to neighboring to find a fiber that is close enough to require inserting a new "tunneling element" into the mesh connectivity. Thus, such a search and insertion process would be practical only after several iterations had eliminated a major percentage of the conducting fibers.

Yet another alternative would be to fit one or more long continuous cables through the retained fibers, even if they contain a gap. As illustrated in Figure 5.1, one can take any reasonable collection of fiber paths and extract their centroid locations and/or their end points to define a general neighborhood of a final continuous path. Then, a particular type of continuous curve, such as a spline, could be least squares fit through those points. The result of such a fitting process would be the single black spline path given in Figure 5.2. Such a process is clearly extendable to three-dimensional paths.
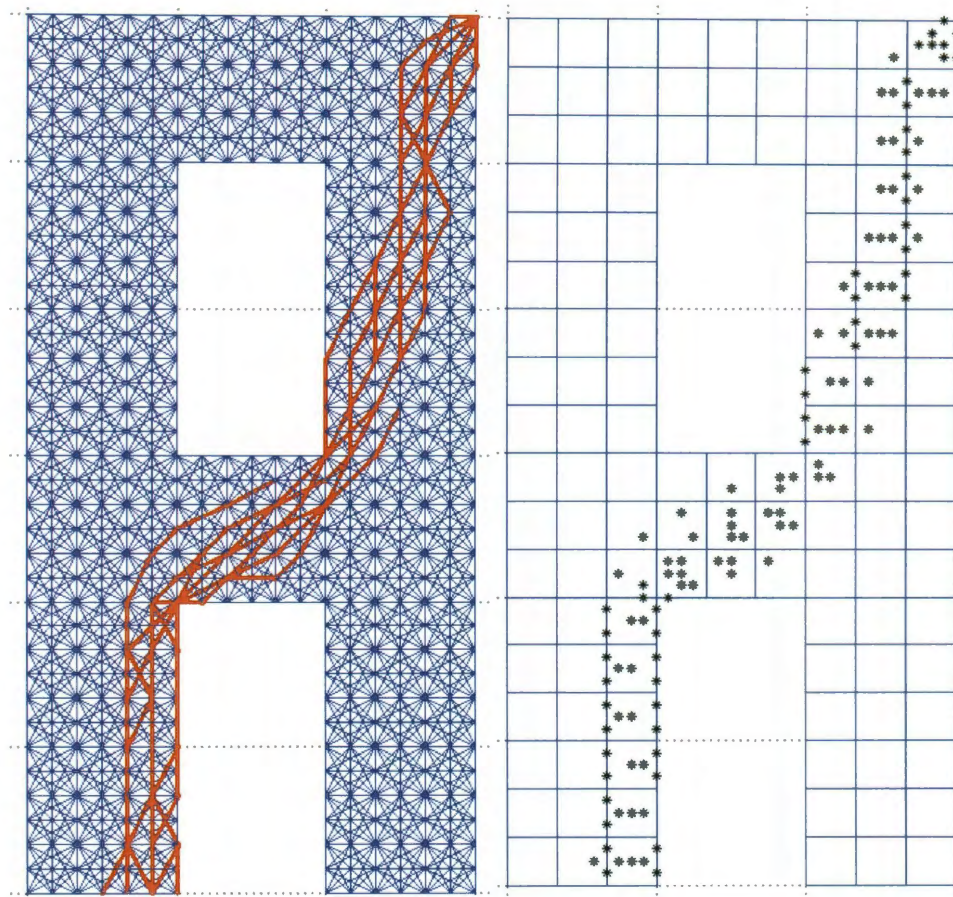
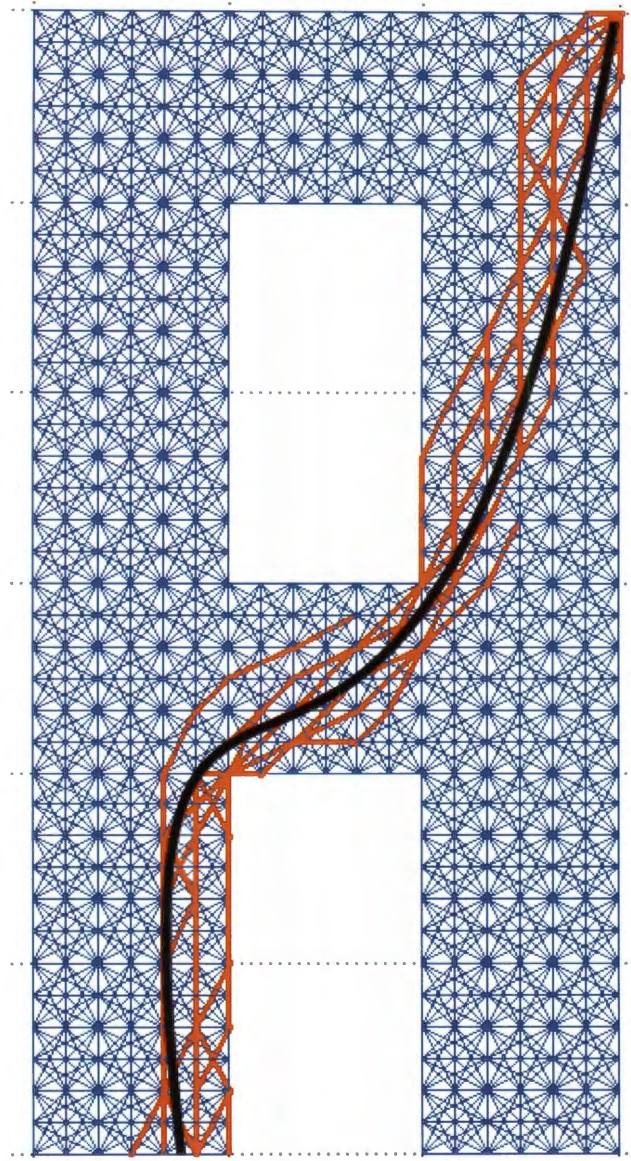Figure 5.1 - Fiber paths (left) and their centroid locations (right)

Figure 5.2 - A single continuous spline curve (black) fit through the retained fibers

Chapter 6

Future Work and Conclusions

6.1. Three-Dimensional Applications

Topological optimization is not necessarily limited to two-dimensional structures, as Hassani and Hinton demonstrate with the three-dimensional control arm example shown in Figure 6.1. In (a), the design (light gray) and non-design (black) domains of the control arm are displayed. Commercial optimization software is used to void elements with low material density in (b), with the final manually smoothed element model for stress analysis shown in (c).

The current fiber optimization methodology can recognize and accept three-dimensional finite element domains such as the control arm example. Fibers would be laid from node-to-node within each cubic element in three-dimensional space. The additional work would occur in the solid element mesh generation phase. For each standard solid element shape, a process similar to that shown in Figure 2.1 would have to be implemented to create the family of initial fibers connecting all of the nodes of the solid elements. A

serendipity quadratic solid element extension, of the left side of that figure, would have 20 nodes. Thus the number of fibers in a solid mesh is drastically increased in the first iteration. The input files become huge, but the algorithm would still function. Visualizing the fibers in a solid domain would not be difficult, but it may be hard to identify where gaps develop in the final few paths.
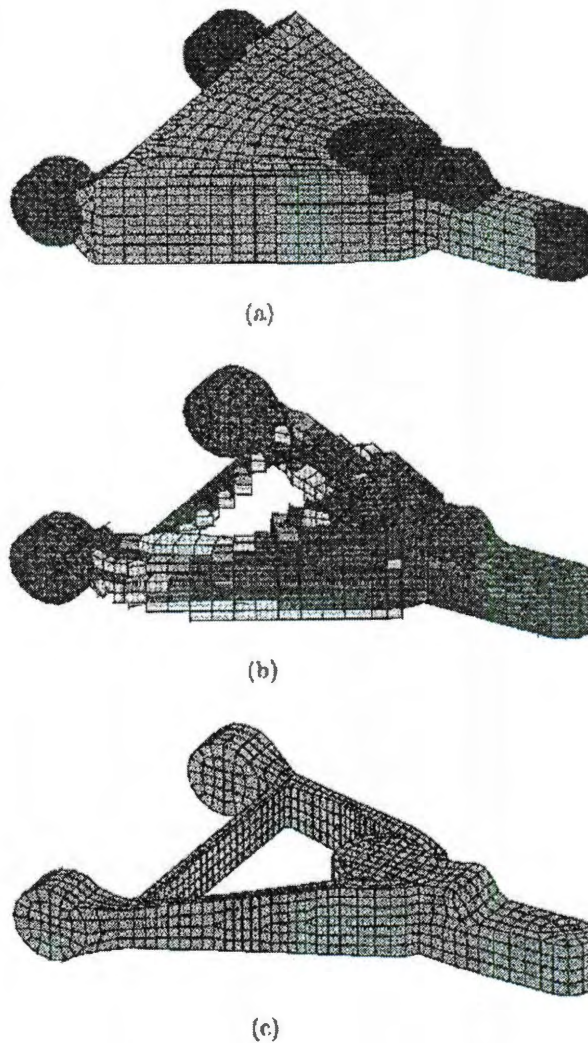

(a)

(b)

(c)

Figure 6.1 - Three-Dimensional Optimization of Control Arm

6.2. Future Work

The speed of the current algorithm can be significantly increased with a few straight forward modifications that merit consideration in the future. Currently, the continuum elements are generated and assembled in every iteration. Since they do not change in the iteration process they only need to be built once. The assembly algorithm could be changed such that before the first iteration all of the continuum elements are formed and assembled first. The assembled stiffness matrix is saved to a high speed binary file. At the beginning of each iteration the equilibrium equations would be initialized by reading in the assemble continuum contribution from the binary file. Then the loop over all fibers would begin. If a fiber had not been deleted then its stiffness is computed and assembled into the equilibrium equations. At the end of the fiber loop, the system would be complete, and the enforcement of the boundary conditions and the final factorizations would take place in the usual fashion. For three-dimensional models this would probably be a necessary step for the process to run in a reasonable time.

6.3. Conclusions

At this current stage, the optimization algorithm for nanofiber placement for improving the mechanical, electrical, or thermal behavior of a structure has been completed. The examples in the study demonstrate both the feasibility of this algorithm, but also potential flaws that can be rectified. This present study, at status quo, serves as the foundation for future research in which a more refined optimization methodology can be realized and extended to fibers in solids. From the results and data obtained, there are a few avenues of research in which the methodology covered here can be improved upon.

While the option to by-pass gaps in the path(s) can be overcome by curve fitting methods (as in Figure 5.2). It would be very useful to have an algorithm that would prevent a fiber from being deleted if it causes a gap in the *last* path. That may not be practical with the current approach because it begins with an extremely large number of paths and it is quite difficult to detect when just a few connected paths remain. The identities of all retained fibers are stored at the end of each iteration. Therefore, one could work backwards and visually identify the last iteration that contained at least one continuous path. Then, you could restart with that fiber connectivity as the initial state, turn on the closed path retention logic, and proceed with deleting fibers that are not on a closed path.

References

[1] S. Amstutz and A. A. Novotny. "Topological Optimization of Structures Subject to Von Mises Stress Constraints." *Structural and Multidisciplinary Optimization* 41.3 (2010): 407-20.

[2] J. A. Baez. *Structural Topology and Shape Optimization Using the Finite Element Method.* PhD Thesis. Rice University (2000). *Rice Digital Scholarship Archive.* Web. 1 Mar. 2011.

[3] M. Beckers and C. Fleury. "A Primal-Dual Approach in Truss Topology Optimization." *Computers and Structures* 64.1-4 (1997): 77-88.

[4] M. Bruyneel. "A general and effective approach for the optimal design of fiber reinforced composite structures." *Composites Science and Technology* 66 (2006): 1303-1314

[5] J. Che, T. Çağın, and W. A. Goddard, III. "Thermal Conductivity of Carbon Nanotubes." *IOPscience, Nanotechnology* 11.2 (2000): 65-69.

[6] G. Cheng, X. Guo, and N. Ofhoff. "New Formulation for Truss Topology Optimization Problems Under Buckling Constraints." *Topology Optimization of Structures and Composite Continua* II 7 (2000): 115-29.

[7] R. D. Cook, *Concepts and Applications of Finite Element Analysis.* John Wiley & Sons, 1974

[8] P. Duysinx, P., and M. P. Bendsøe. "Topology Optimization of Continuum Structures with Local Stress Constraints." *International Journal for Numerical Methods in Engineering* 43.8 (1998): 1453-478.

[9] P. Elsbernd. "A Non-Linear Finite Element Model for the Determination of Elastic and Thermal Properties of Nanocomposites." MS Thesis. Rice University (2009).

[10] M. Esteva. "Hybrid Finite Elements Nanocomposite Characterization by Stochastic Microstructuring." PhD Thesis. Rice University (2008)

[11] S. M. Giusti, A. A. Novotny, and J. Sokolowski. "Topological Derivative for Steady-state Orthotropic Heat Diffusion Problem." *Structural and Multidisciplinary Optimization* 40.1-6 (2010): 53-64.

[12] P. Hajela, and E. Lee. "Genetic Algorithms in Truss Topological Optimization." *International Journal of Solids and Structures* 32.22 (1995): 3341-357.

[13] P. Hajela and S. Vittal. "Evolutionary Computing and Structural Topology Optimization - A State of the Art Assessment." *Topology Optimization of Structures and Composite Continua* II 7 (2000): 195-209.

[14] B. Hassani, and E. Hinton. *Homogenization and Structural Topology Optimization: Theory, Practice, and Software*. London: Springer, 1999.

[15] M. R. Islam, and A. Pramila. "Thermal Conductivity of Fiber Reinforced Composites by the FEM." *Journal of Composite Materials* 33.18 (1999): 1699-715.

[16] M. Kamiński. "Homogenization of transient heat transfer problems for some composite materials." *International Journal of Engineering Science* 41 (2003). 1-29

[17] D. W. Kelly, C. A. Reidsema, and M. C. W. Lee. "An algorithm for defining load paths and load bearing topology in finite element analysis." *Engineering Computations: International Journal for Computer-Aided Engineering and Software* 28.2 (2011). 196-214

[18] A. V. Kumar, and A. Parthasarathy. "Topology Optimization Using B-spline Finite Elements." *Structural and Multidisciplinary Optimization* (2011).

[19] Q. Li, G. P. Steven, O. M. Querin, and Y. M. Xie. "Shape and Topology Design for Heat Conduction by Evolutionary Structural Optimization." *International Journal of Heat and Mass Transfer* 42.17 (1999): 3361-371.

[20] O. M. Querin, G. P. Steven, and Y. M. Xie. "Advances in Evolutionary Structural Optimisation: 1992-2000." *Topology Optimization of Structures and Composite Continua* II 7 (2000): 227-36.

[21] G. I. N. Rozvany. "Problem Classes, Solution Strategies, and Unified Terminology of FE-Based Topology Optimization." *Topology Optimization of Structures and Composite Continua* II 7 (2000): 19-35

[22] O. Sigmund. "A 99 Line Topology Optimization Code Written in Matlab." *Structural and Multidisciplinary Optimization* 21.2 (2001): 120-27.

[23] P. Tanskanen. "The Evolutionary Structural Optimization Method: Theoretical Aspects." *Computer Methods in Applied Mechanics and Engineering* 191.47-48 (2002): 5485-498.

[24] W. Waldman, M. Heller, R. Kaye, and F. Rose. "Advances in two-dimensional structural loadflow visualisation." *Engineering Computations: International Journal for Computer-Aided Engineering and Software* 19.3 (2002). 305-326

[25] M. Wichmann. *Numerical Modeling, Determination, and Characterization of Electrical Properties of Nanocomposites*. MS Thesis. Rice University (2011)

[26] S. Wu, T. Natsuki, K. Kurashiki, Q. Ni, M. Iwamoto, and Y. Fujii. "Conductivity Stability of Carbon Nanofiber/unsaturated Polyester Nanocomposites." *Advanced Composite Materials* 16.3 (2007): 195-206.

[27] Y. Xie, and G. Steven. "A Simple Evolutionary Procedure for Structural Optimization." *Computers & Structures* 49.5 (1993): 885-96.

[28] K. Zhou, and X. Li. "Topology Optimization of Structures Under Multiple Load Cases Using a Fiber-reinforced Composite Material Model." *Computational Mechanics* 38.2 (2006): 163-70.